Appl. Math. Mech. -Engl. Ed., **35**(8), 1005–1028 (2014)
DOI 10.1007/s10483-014-1846-7

Applied Mathematics and Mechanics (English Edition)

Line-integral representations for extended displacements, stresses, and interaction energy of arbitrary dislocation loops in transversely isotropic magneto-electro-elastic bimaterials*

Jiang-hong YUAN (袁江宏)[1], Wei-qiu CHEN (陈伟球)[2], E. PAN[3]

(1. Department of Civil Engineering, Zhejiang University, Hangzhou 310058, P. R. China;
2. Department of Engineering Mechanics, Zhejiang University, Hangzhou 310027, P. R. China;
3. Department of Civil Engineering and Department of Applied Mathematics, University of Akron, Akron, OH 44325, U. S. A.)

Abstract In addition to the hexagonal crystals of class 6 mm, many piezoelectric materials (e.g., $BaTiO_3$), piezomagnetic materials (e.g., $CoFe_2O_4$), and multiferroic composite materials (e.g., $BaTiO_3$-$CoFe_2O_4$ composites) also exhibit symmetry of transverse isotropy after poling, with the isotropic plane perpendicular to the poling direction. In this paper, simple and elegant line-integral expressions are derived for extended displacements, extended stresses, self-energy, and interaction energy of arbitrarily shaped, three-dimensional (3D) dislocation loops with a constant extended Burgers vector in transversely isotropic magneto-electro-elastic (MEE) bimaterials (i.e., joined half-spaces). The derived solutions can also be simply reduced to those expressions for piezoelectric, piezomagnetic, or purely elastic materials. Several numerical examples are given to show both the multi-field coupling effect and the interface/surface effect in transversely isotropic MEE materials.

Key words dislocation loop, multiferroic, transverse isotropy, bimaterial, half space, extended displacement, extended stress, interaction energy

Chinese Library Classification O343.8
2010 Mathematics Subject Classification 74E10, 74F15, 74M25

1 Introduction

The magneto-electro-elastic (MEE) or multiferroic composite materials, which exhibit the multi-field couplings among the elastic, electric, and magnetic fields, have recently stimulated a great deal of scientific research for their potential applications to the multifunctional devices such as memories, harvesters, sensors, transducers, and actuators[1–2]. MEE materials are usually composites made of multi-phases or multi-layers, such as particulate composites, rod-array composites, and laminate composites[1]. The desirable magneto-electric (ME) coupling usually arises from the strain-mediated elastic interaction across piezomagnetic-piezoelectric interfaces[1–2]. Therefore, the interfaces can have a great influence on the property of MEE

* Received Sept. 6, 2013 / Revised Nov. 29, 2013
Project supported by the National Project of Scientific and Technical Supporting Programs Funded by Ministry of Science & Technology of China (No. 2009BAG12A01-A03-2) and the National Natural Science Foundation of China (Nos. 10972196, 11090333, 11172273, and 11321202)
Corresponding author E. PAN, Professor, Ph. D., E-mail: pan2@uakron.edu

materials and the performance of MEE devices. At the same time, as common defects in crystalline solids, dislocations inevitably interact with the microstructures and interfaces of the MEE materials and therefore affect the mechanical, electrical, and magnetic properties of MEE materials. Due to the above facts, it is necessary to investigate the interaction of dislocations with interfaces in MEE composite materials.

For the problem of dislocation-interface interactions, most related work in the literature is confined to purely elastic materials[3–8]. Little work has been done to treat the interaction of an arbitrary three-dimensional (3D) dislocation loop with the interface/surface of MEE composite materials. Recently, Han et al.[9] derived analytical expressions of the extended displacements and extended stresses induced by a planar dislocation loop of arbitrary shape in a generally anisotropic MEE bimaterial. As an extension to our recent work[3], by utilizing the potential theory, in this paper we mainly solve the extended displacements and extended stresses due to a 3D dislocation loop of arbitrary shape, and the interaction energy between two arbitrarily shaped 3D dislocation loops in transversely isotropic MEE bimaterials. The MEE bimaterial considered here is composed of two dissimilar semi-infinite transversely isotropic MEE solids, which are perfectly bonded together at a planar interface. We assume that the bimaterial interface is parallel to the isotropic plane of both MEE solids (i.e., perpendicular to the poling direction of both MEE solids).

The present paper is organized as follows. In Section 2, we express the point-force Green's function for the non-degenerate transversely isotropic MEE bimaterials in a new way for the sake of later derivations of the dislocation solutions. In Section 3, using Green's function method, we derive line-integral expressions for the extended displacements and extended stresses of an arbitrary 3D dislocation loop, and the interaction energy between two arbitrary 3D dislocation loops in transversely isotropic MEE bimaterials. In Section 4, we provide several numerical examples to show the multi-field coupling effect and the influence of material interface/surface on the extended displacements, extended stresses, and interaction energy of dislocation loops. Concluding remarks are drawn in Section 5.

2 Point-force Green's function for transversely isotropic MEE bimaterials

Before the discussion, it would be pointed out that throughout the paper we follow the conventions below: (i) The range of Roman indices is from 1 to 3 for lowercase letters (i, j, k, etc.) and from 1 to 5 for uppercase letters (I, J, K, etc.), and the range of Greek indices (α, β, γ, etc.) is from 1 to 2, unless otherwise specified. (ii) When dealing with bimaterials, the Greek index λ or μ in the square bracket (i.e., $[\lambda]$ or $[\mu]$) indicates the corresponding relationship with material λ or material μ.

In the Cartesian coordinates (x_1, x_2, x_3), we consider a bimaterial which is composed of two joined half-spaces, as shown in Fig. 1(a). In this bimaterial, one half-space ($x_3 >0$) is occupied by transversely isotropic MEE material 1, and the other half-space ($x_3 <0$) is occupied by transversely isotropic MEE material 2. The two half-spaces are perfectly bonded together at the planar interface (x_3=0), which means that both the extended displacements u_I and the extended stresses σ_{3J} are continuous at x_3=0 (the extended displacement and extended stress are defined in (A2)). We further assume that the isotropic plane of each material is parallel to the bimaterial interface (x_3=0).

We denote the point-force Green's function for transversely isotropic MEE bimaterials as $u_{IJ}^{[\lambda][\mu]}(\boldsymbol{y};\boldsymbol{x})$, which means the Ith component of the extended displacement at point $\boldsymbol{y}\,(y_1,\, y_2,\, y_3)$ in material λ due to the Jth component (of unit magnitude) of the extended body force applied at point $\boldsymbol{x}\,(x_1,\, x_2,\, x_3)$ in material μ (the extended body force is defined in (A2)). By virtue of the image method, the point-force Green's function for bimaterials can be divided into two parts as follows:

$$u_{IJ}^{[\lambda][\mu]}(\boldsymbol{y};\boldsymbol{x})=\delta_{\lambda\mu}u_{IJ}^{[\mu]}(\boldsymbol{y};\boldsymbol{x})+U_{IJ}^{[\lambda][\mu]}(\boldsymbol{y};\boldsymbol{x}),\tag{1}$$

where $u_{IJ}^{[\mu]}(\boldsymbol{y};\boldsymbol{x})$ is the point-force Green's function for the transversely isotropic MEE full space occupied by material μ, while $U_{IJ}^{[\lambda][\mu]}(\boldsymbol{y};\boldsymbol{x})$ is the complementary part from the image sources due to the bimaterial interface; δ_{ij} is the 3×3 Kronecker delta defined as

$$\delta_{ij}=\begin{cases}1, & i=j,\\ 0, & i\neq j.\end{cases}\tag{2}$$

According to the reciprocity theorem in linear magneto-electro-elasticity[10], we can find that

$$\begin{cases}u_{IJ}^{[\mu]}(\boldsymbol{y};\boldsymbol{x})=u_{JI}^{[\mu]}(\boldsymbol{x};\boldsymbol{y})=u_{JI}^{[\mu]}(\boldsymbol{y};\boldsymbol{x}),\\ U_{IJ}^{[\lambda][\mu]}(\boldsymbol{y};\boldsymbol{x})=U_{JI}^{[\mu][\lambda]}(\boldsymbol{x};\boldsymbol{y}).\end{cases}\tag{3}$$

For the sake of later derivations, we now express $u_{IJ}^{[\mu]}(\boldsymbol{y};\boldsymbol{x})$ and $U_{IJ}^{[\lambda][\mu]}(\boldsymbol{y};\boldsymbol{x})$ in terms of second derivatives of certain potential functions as follows:

$$\begin{pmatrix}u_{IJ}^{[\mu]}(\boldsymbol{y};\boldsymbol{x})\\ U_{IJ}^{[\lambda][\mu]}(\boldsymbol{y};\boldsymbol{x})\end{pmatrix}=\frac{1}{4\pi c_{44}^{[\mu]}}\frac{\partial^2}{\partial y_I\partial x_J}\begin{pmatrix}\Psi_{IJ}^{[\mu]}(\boldsymbol{y};\boldsymbol{x})\\ \Psi_{IJ}^{[\lambda][\mu]}(\boldsymbol{y};\boldsymbol{x})\end{pmatrix}+\frac{\delta_{IJ}}{4\pi c_{44}^{[\mu]}}\frac{\partial^2}{\partial x_3^2}\begin{pmatrix}\Phi_{I}^{[\mu]}(\boldsymbol{y};\boldsymbol{x})\\ \Phi_{I}^{[\lambda][\mu]}(\boldsymbol{y};\boldsymbol{x})\end{pmatrix},\tag{4}$$

where

$$\begin{cases}\begin{pmatrix}\Psi_{\xi\eta}^{[\mu]}(\boldsymbol{y};\boldsymbol{x})\\ \Psi_{\xi\eta}^{[\lambda][\mu]}(\boldsymbol{y};\boldsymbol{x})\end{pmatrix}=\begin{pmatrix}\psi_{1}^{[\mu]}(\boldsymbol{y};\boldsymbol{x})-\psi_{5}^{[\mu]}(\boldsymbol{y};\boldsymbol{x})\\ \psi_{1}^{[\lambda][\mu]}(\boldsymbol{y};\boldsymbol{x})-\psi_{5}^{[\lambda][\mu]}(\boldsymbol{y};\boldsymbol{x})\end{pmatrix},\\ \begin{pmatrix}\Psi_{(i+2)\eta}^{[\mu]}(\boldsymbol{y};\boldsymbol{x})\\ \Psi_{(i+2)\eta}^{[\lambda][\mu]}(\boldsymbol{y};\boldsymbol{x})\end{pmatrix}=\begin{pmatrix}\psi_{2;i}^{[\mu]}(\boldsymbol{y};\boldsymbol{x})\\ \psi_{2;i}^{[\lambda][\mu]}(\boldsymbol{y};\boldsymbol{x})\end{pmatrix},\\ \begin{pmatrix}\Psi_{\xi(j+2)}^{[\mu]}(\boldsymbol{y};\boldsymbol{x})\\ \Psi_{\xi(j+2)}^{[\lambda][\mu]}(\boldsymbol{y};\boldsymbol{x})\end{pmatrix}=\begin{pmatrix}\psi_{3;j}^{[\mu]}(\boldsymbol{y};\boldsymbol{x})\\ \psi_{3;j}^{[\lambda][\mu]}(\boldsymbol{y};\boldsymbol{x})\end{pmatrix},\\ \begin{pmatrix}\Psi_{(i+2)(j+2)}^{[\mu]}(\boldsymbol{y};\boldsymbol{x})\\ \Psi_{(i+2)(j+2)}^{[\lambda][\mu]}(\boldsymbol{y};\boldsymbol{x})\end{pmatrix}=\begin{pmatrix}\psi_{4;ij}^{[\mu]}(\boldsymbol{y};\boldsymbol{x})\\ \psi_{4;ij}^{[\lambda][\mu]}(\boldsymbol{y};\boldsymbol{x})\end{pmatrix},\end{cases}\tag{5a}$$

and

$$\begin{pmatrix}\Phi_{\xi}^{[\mu]}(\boldsymbol{y};\boldsymbol{x})\\ \Phi_{\xi}^{[\lambda][\mu]}(\boldsymbol{y};\boldsymbol{x})\end{pmatrix}=(\gamma_5^{[\mu]})^2\begin{pmatrix}\psi_{5}^{[\mu]}(\boldsymbol{y};\boldsymbol{x})\\ \psi_{5}^{[\lambda][\mu]}(\boldsymbol{y};\boldsymbol{x})\end{pmatrix},\quad \begin{pmatrix}\Phi_{i+2}^{[\mu]}(\boldsymbol{y};\boldsymbol{x})\\ \Phi_{i+2}^{[\lambda][\mu]}(\boldsymbol{y};\boldsymbol{x})\end{pmatrix}=\begin{pmatrix}0\\ 0\end{pmatrix}.\tag{5b}$$

In (4) and (5b), the material constants $c_{44}^{[\mu]}$ and $\gamma_5^{[\mu]}$ are defined in (A3b) and (A6), respectively. In (4), the extended partial derivative is defined as follows:

$$\frac{\partial}{\partial y_I}=\begin{cases}\dfrac{\partial}{\partial y_i}, & I=i=1,2,3,\\ \dfrac{\partial}{\partial y_3}, & I=4,5,\end{cases}\qquad \frac{\partial}{\partial x_I}=\begin{cases}\dfrac{\partial}{\partial x_i}, & I=i=1,2,3,\\ \dfrac{\partial}{\partial x_3}, & I=4,5,\end{cases}\tag{6a}$$

and the extended Kronecker delta is defined as

$$\delta_{IJ}=\begin{cases}\delta_{ij}, & I=i=1,2,3,\quad J=j=1,2,3,\\ \delta_{i3}, & I=i=1,2,3,\quad J=4,5,\\ \delta_{3j}, & I=4,5,\quad J=j=1,2,3,\\ 1, & I=4,5,\quad J=4,5.\end{cases}\tag{6b}$$

Similarly, for easy use in this paper, we further define the extended differential as

$$\mathrm{d}y_I = \begin{cases} \mathrm{d}y_i, & I = i = 1, 2, 3, \\ \mathrm{d}y_3, & I = 4, 5, \end{cases} \qquad \mathrm{d}x_I = \begin{cases} \mathrm{d}x_i, & I = i = 1, 2, 3, \\ \mathrm{d}x_3, & I = 4, 5, \end{cases} \tag{6c}$$

and the extended permutation symbol as

$$\varepsilon_{IJK} = \begin{cases} \varepsilon_{ijk}, & I = i = 1, 2, 3, \quad J = j = 1, 2, 3, \quad K = k = 1, 2, 3, \\ \varepsilon_{3jk}, & I = 4, 5, \quad J = j = 1, 2, 3, \quad K = k = 1, 2, 3, \\ \varepsilon_{i3k}, & J = 4, 5, \quad K = k = 1, 2, 3, \quad I = i = 1, 2, 3, \\ \varepsilon_{ij3}, & K = 4, 5, \quad I = i = 1, 2, 3, \quad J = j = 1, 2, 3, \\ 0, & \text{otherwise}, \end{cases} \tag{6d}$$

where ε_{ijk} is the classic permutation symbol defined as

$$\varepsilon_{ijk} = \begin{cases} +1, & (i, j, k) = (1, 2, 3), (2, 3, 1), (3, 1, 2), \\ -1, & (i, j, k) = (1, 3, 2), (3, 2, 1), (2, 1, 3), \\ 0, & \text{otherwise}. \end{cases} \tag{7}$$

Based upon the general solutions of the coupled equations for transversely isotropic MEE media summarized in Appendix A[11−12], the unknown functions in (5a) and (5b) for the non-degenerate bimaterials are found to be

$$\begin{pmatrix} \psi_5^{[\mu]}(\boldsymbol{y};\boldsymbol{x}) \\ \psi_5^{[\lambda][\mu]}(\boldsymbol{y};\boldsymbol{x}) \end{pmatrix} \triangleq \begin{pmatrix} \psi_5^{[\mu]} \\ \psi_5^{[\lambda][\mu]} \end{pmatrix} = \gamma_5^{[\mu]} \begin{pmatrix} \chi_5^{[\mu]}(\boldsymbol{y};\boldsymbol{x}) \\ p_{55}^{[\lambda][\mu]} \chi_{55}^{[\lambda][\mu]}(\boldsymbol{y};\boldsymbol{x}) \end{pmatrix}, \tag{8a}$$

and

$$\begin{cases} \begin{pmatrix} \psi_1^{[\mu]}(\boldsymbol{y};\boldsymbol{x}) \\ \psi_1^{[\lambda][\mu]}(\boldsymbol{y};\boldsymbol{x}) \end{pmatrix} \triangleq \begin{pmatrix} \psi_1^{[\mu]} \\ \psi_1^{[\lambda][\mu]} \end{pmatrix} = \sum\limits_{n=1}^{4} H_n^{[\mu]} \begin{pmatrix} \chi_n^{[\mu]}(\boldsymbol{y};\boldsymbol{x}) \\ \sum\limits_{m=1}^{4} p_{mn}^{[\lambda][\mu]} \chi_{mn}^{[\lambda][\mu]}(\boldsymbol{y};\boldsymbol{x}) \end{pmatrix}, \\ \begin{pmatrix} \psi_{2;i}^{[\mu]}(\boldsymbol{y};\boldsymbol{x}) \\ \psi_{2;i}^{[\lambda][\mu]}(\boldsymbol{y};\boldsymbol{x}) \end{pmatrix} \triangleq \begin{pmatrix} \psi_{2;i}^{[\mu]} \\ \psi_{2;i}^{[\lambda][\mu]} \end{pmatrix} = \sum\limits_{n=1}^{4} H_n^{[\mu]} \begin{pmatrix} m_{ni}^{[\mu]} \chi_n^{[\mu]}(\boldsymbol{y};\boldsymbol{x}) \\ \sum\limits_{m=1}^{4} m_{mi}^{[\lambda]} p_{mn}^{[\lambda][\mu]} \chi_{mn}^{[\lambda][\mu]}(\boldsymbol{y};\boldsymbol{x}) \end{pmatrix}, \\ \begin{pmatrix} \psi_{3;j}^{[\mu]}(\boldsymbol{y};\boldsymbol{x}) \\ \psi_{3;j}^{[\lambda][\mu]}(\boldsymbol{y};\boldsymbol{x}) \end{pmatrix} \triangleq \begin{pmatrix} \psi_{3;j}^{[\mu]} \\ \psi_{3;j}^{[\lambda][\mu]} \end{pmatrix} = \sum\limits_{n=1}^{4} H_n^{[\mu]} \begin{pmatrix} m_{nj}^{[\mu]} \chi_n^{[\mu]}(\boldsymbol{y};\boldsymbol{x}) \\ \sum\limits_{m=1}^{4} m_{nj}^{[\mu]} p_{mn}^{[\lambda][\mu]} \chi_{mn}^{[\lambda][\mu]}(\boldsymbol{y};\boldsymbol{x}) \end{pmatrix}, \\ \begin{pmatrix} \psi_{4;ij}^{[\mu]}(\boldsymbol{y};\boldsymbol{x}) \\ \psi_{4;ij}^{[\lambda][\mu]}(\boldsymbol{y};\boldsymbol{x}) \end{pmatrix} \triangleq \begin{pmatrix} \psi_{4;ij}^{[\mu]} \\ \psi_{4;ij}^{[\lambda][\mu]} \end{pmatrix} = \sum\limits_{n=1}^{4} H_n^{[\mu]} \begin{pmatrix} m_{ni}^{[\mu]} m_{nj}^{[\mu]} \chi_n^{[\mu]}(\boldsymbol{y};\boldsymbol{x}) \\ \sum\limits_{m=1}^{4} m_{mi}^{[\lambda]} m_{nj}^{[\mu]} p_{mn}^{[\lambda][\mu]} \chi_{mn}^{[\lambda][\mu]}(\boldsymbol{y};\boldsymbol{x}) \end{pmatrix}. \end{cases} \tag{8b}$$

In (8b), the material constant $m_{nj}^{[\mu]}$ $(n = 1, 2, 3, 4)$ is defined in (A11). In (8a) and (8b), the symbol "$\triangleq$" means that, without confusion, $\psi_*^{[\mu]}(\boldsymbol{y};\boldsymbol{x})$ and $\psi_*^{[\lambda][\mu]}(\boldsymbol{y};\boldsymbol{x})$ can be written as $\psi_*^{[\mu]}$ and $\psi_*^{[\lambda][\mu]}$ for short, respectively. From (8b), we can further obtain the following useful relations:

$$\psi_{2;i}^{[\mu]} = \psi_{3;i}^{[\mu]}, \quad \psi_{4;ij}^{[\mu]} = \psi_{4;ji}^{[\mu]}. \tag{9}$$

For the bimaterial with a perfectly-bonded interface, the unknown coefficients in (8a) and (8b) are determined by[11]

$$\begin{pmatrix} H_1^{[\mu]} \\ H_2^{[\mu]} \\ H_3^{[\mu]} \\ H_4^{[\mu]} \end{pmatrix} = \begin{pmatrix} s_1^{[\mu]} & s_2^{[\mu]} & s_3^{[\mu]} & s_4^{[\mu]} \\ \alpha_{11}^{[\mu]} & \alpha_{21}^{[\mu]} & \alpha_{31}^{[\mu]} & \alpha_{41}^{[\mu]} \\ \alpha_{12}^{[\mu]} & \alpha_{22}^{[\mu]} & \alpha_{32}^{[\mu]} & \alpha_{42}^{[\mu]} \\ \alpha_{13}^{[\mu]} & \alpha_{23}^{[\mu]} & \alpha_{33}^{[\mu]} & \alpha_{43}^{[\mu]} \end{pmatrix}^{-1} \begin{pmatrix} 1 \\ 0 \\ 0 \\ 0 \end{pmatrix}, \tag{10}$$

$$\begin{pmatrix} p_{55}^{[\mu][\mu]} \\ p_{55}^{[3-\mu][\mu]} \end{pmatrix} = \begin{pmatrix} 1 & -1 \\ c_{44}^{[\mu]} s_5^{[\mu]} & c_{44}^{[3-\mu]} s_5^{[3-\mu]} \end{pmatrix}^{-1} \begin{pmatrix} -1 \\ c_{44}^{[\mu]} s_5^{[\mu]} \end{pmatrix}, \tag{11a}$$

and

$$\begin{aligned} \begin{pmatrix} p_{1n}^{[\mu][\mu]} \\ p_{2n}^{[\mu][\mu]} \\ p_{3n}^{[\mu][\mu]} \\ p_{4n}^{[\mu][\mu]} \\ p_{1n}^{[3-\mu][\mu]} \\ p_{2n}^{[3-\mu][\mu]} \\ p_{3n}^{[3-\mu][\mu]} \\ p_{4n}^{[3-\mu][\mu]} \end{pmatrix} = & \begin{pmatrix} 1 & 1 & 1 & 1 & -1 & -1 & -1 & -1 \\ \alpha_{11}^{[\mu]} & \alpha_{21}^{[\mu]} & \alpha_{31}^{[\mu]} & \alpha_{41}^{[\mu]} & \alpha_{11}^{[3-\mu]} & \alpha_{21}^{[3-\mu]} & \alpha_{31}^{[3-\mu]} & \alpha_{41}^{[3-\mu]} \\ \alpha_{12}^{[\mu]} & \alpha_{22}^{[\mu]} & \alpha_{32}^{[\mu]} & \alpha_{42}^{[\mu]} & \alpha_{12}^{[3-\mu]} & \alpha_{22}^{[3-\mu]} & \alpha_{32}^{[3-\mu]} & \alpha_{42}^{[3-\mu]} \\ \alpha_{13}^{[\mu]} & \alpha_{23}^{[\mu]} & \alpha_{33}^{[\mu]} & \alpha_{43}^{[\mu]} & \alpha_{13}^{[3-\mu]} & \alpha_{23}^{[3-\mu]} & \alpha_{33}^{[3-\mu]} & \alpha_{43}^{[3-\mu]} \\ \omega_{11}^{[\mu]} & \omega_{21}^{[\mu]} & \omega_{31}^{[\mu]} & \omega_{41}^{[\mu]} & \omega_{11}^{[3-\mu]} & \omega_{21}^{[3-\mu]} & \omega_{31}^{[3-\mu]} & \omega_{41}^{[3-\mu]} \\ \theta_{11}^{[\mu]} & \theta_{21}^{[\mu]} & \theta_{31}^{[\mu]} & \theta_{41}^{[\mu]} & -\theta_{11}^{[3-\mu]} & -\theta_{21}^{[3-\mu]} & -\theta_{31}^{[3-\mu]} & -\theta_{41}^{[3-\mu]} \\ \theta_{12}^{[\mu]} & \theta_{22}^{[\mu]} & \theta_{32}^{[\mu]} & \theta_{42}^{[\mu]} & -\theta_{12}^{[3-\mu]} & -\theta_{22}^{[3-\mu]} & -\theta_{32}^{[3-\mu]} & -\theta_{42}^{[3-\mu]} \\ \theta_{13}^{[\mu]} & \theta_{23}^{[\mu]} & \theta_{33}^{[\mu]} & \theta_{43}^{[\mu]} & -\theta_{13}^{[3-\mu]} & -\theta_{23}^{[3-\mu]} & -\theta_{33}^{[3-\mu]} & -\theta_{43}^{[3-\mu]} \end{pmatrix}^{-1} \\ & \cdot \begin{pmatrix} -1 \\ \alpha_{n1}^{[\mu]} \\ \alpha_{n2}^{[\mu]} \\ \alpha_{n3}^{[\mu]} \\ \omega_{n1}^{[\mu]} \\ -\theta_{n1}^{[\mu]} \\ -\theta_{n2}^{[\mu]} \\ -\theta_{n3}^{[\mu]} \end{pmatrix} \quad (n = 1, 2, 3, 4), \end{aligned} \tag{11b}$$

in which the material constants $s_J^{[\mu]}$, $\alpha_{nj}^{[\mu]}$, $\omega_{nj}^{[\mu]}$, and $\theta_{nj}^{[\mu]}$ $(n = 1, 2, 3, 4)$ are defined in (A6) and (A11), respectively.

Also in (8a) and (8b), the unknown functions are defined as[13–14]

$$\chi_J^{[\mu]}(\boldsymbol{y};\boldsymbol{x}) \triangleq \chi_J^{[\mu]} = \begin{cases} z_J^{[\mu]} \ln(R_J^{[\mu]} + z_J^{[\mu]}) - R_J^{[\mu]} & \text{if} \quad R_J^{[\mu]} + z_J^{[\mu]} \neq 0, \\ -z_J^{[\mu]} \ln(R_J^{[\mu]} - z_J^{[\mu]}) - R_J^{[\mu]} & \text{if} \quad R_J^{[\mu]} + z_J^{[\mu]} = 0, \end{cases}$$

or

$$\chi_J^{[\mu]}(\boldsymbol{y};\boldsymbol{x}) = \begin{cases} -z_J^{[\mu]} \ln(R_J^{[\mu]} - z_J^{[\mu]}) - R_J^{[\mu]} & \text{if} \quad R_J^{[\mu]} - z_J^{[\mu]} \neq 0, \\ z_J^{[\mu]} \ln(R_J^{[\mu]} + z_J^{[\mu]}) - R_J^{[\mu]} & \text{if } R_J^{[\mu]} - z_J^{[\mu]} = 0, \end{cases} \tag{12}$$

$$\chi_{IJ}^{[\lambda][\mu]}(\boldsymbol{y};\boldsymbol{x}) \triangleq \chi_{IJ}^{[\lambda][\mu]} = z_{IJ}^{[\lambda][\mu]} \ln(R_{IJ}^{[\lambda][\mu]} + z_{IJ}^{[\lambda][\mu]}) - R_{IJ}^{[\lambda][\mu]},$$

where

$$\begin{cases} R_J^{[\mu]} = R_J^{[\mu]}(\boldsymbol{y};\boldsymbol{x}) = \sqrt{(y_1-x_1)^2+(y_2-x_2)^2+(z_J^{[\mu]})^2}, \\ R_{IJ}^{[\lambda][\mu]} = R_{IJ}^{[\lambda][\mu]}(\boldsymbol{y};\boldsymbol{x}) = \sqrt{(y_1-x_1)^2+(y_2-x_2)^2+(z_{IJ}^{[\lambda][\mu]})^2}, \end{cases} \tag{13}$$

$$\begin{cases} z_J^{[\mu]} = z_J^{[\mu]}(\boldsymbol{y};\boldsymbol{x}) = s_J^{[\mu]}(y_3-x_3), \\ z_{IJ}^{[\lambda][\mu]} = z_{IJ}^{[\lambda][\mu]}(\boldsymbol{y};\boldsymbol{x}) = (-1)^{\lambda+1}s_I^{[\lambda]}y_3+(-1)^{\mu+1}s_J^{[\mu]}x_3. \end{cases} \tag{14}$$

The functions defined in (12) satisfy the following useful relations:

$$\begin{cases} (\gamma_J^{[\mu]})^2\dfrac{\partial^2}{\partial y_3^2}\chi_J^{[\mu]} = -\Big(\dfrac{\partial^2}{\partial y_1^2}+\dfrac{\partial^2}{\partial y_2^2}\Big)\chi_J^{[\mu]} = \dfrac{1}{R_J^{[\mu]}}, \\ (\gamma_I^{[\lambda]})^2\dfrac{\partial^2}{\partial y_3^2}\chi_{IJ}^{[\lambda][\mu]} = -\Big(\dfrac{\partial^2}{\partial y_1^2}+\dfrac{\partial^2}{\partial y_2^2}\Big)\chi_{IJ}^{[\lambda][\mu]} = \dfrac{1}{R_{IJ}^{[\lambda][\mu]}}, \end{cases} \tag{15}$$

and

$$\begin{cases} \dfrac{\partial}{\partial y_i}\chi_J^{[\mu]} = -\dfrac{\partial}{\partial x_i}\chi_J^{[\mu]}\,, \quad \dfrac{\partial}{\partial y_\xi}\chi_{IJ}^{[\lambda][\mu]} = -\dfrac{\partial}{\partial x_\xi}\chi_{IJ}^{[\lambda][\mu]}, \\ \dfrac{\partial}{\partial y_3}\chi_{IJ}^{[\lambda][\mu]} = (-1)^{\lambda+\mu}s_I^{[\lambda]}\gamma_J^{[\mu]}\dfrac{\partial}{\partial x_3}\chi_{IJ}^{[\lambda][\mu]}. \end{cases} \tag{16}$$

3 Line-integral forms of extended displacements, stresses, and interaction energy of arbitrarily shaped 3D dislocation loops in transversely isotropic MEE bimaterials

3.1 Extended displacements of arbitrarily shaped 3D dislocation loop

Now, we consider an arbitrarily shaped 3D dislocation loop C bounding a curved surface A in transversely isotropic MEE bimaterials (see Fig. 1(b)). Based upon the classical theory of dislocations, the extended displacements induced by this dislocation loop can be expressed as[15]

$$u_N^{[\mu][\lambda]}(\boldsymbol{x}) = -\sum_{J,K=1}^{5}\sum_{i,l=1}^{3}\int_A \mathrm{d}A_i b_J c_{iJKl}^{[\lambda]}\frac{\partial}{\partial y_l}u_{KN}^{[\lambda][\mu]}(\boldsymbol{y};\boldsymbol{x}), \tag{17}$$

where $u_N^{[\mu][\lambda]}(\boldsymbol{x})$ is the Nth component of the extended displacement at point $\boldsymbol{x}$ $(x_1,\ x_2,\ x_3)$ in material μ due to the dislocation loop C located in material λ, $\mathrm{d}A_i$ at point $\boldsymbol{y}\,(y_1,\ y_2,\ y_3)$ is the ith component of the vector area element $\mathrm{d}\boldsymbol{A}$, and the positive normal of $\mathrm{d}\boldsymbol{A}$ is associated with the positive direction of the closed dislocation line according to the right-hand rule (Fig. 1(b)), the extended elastic coefficient tensor $c_{iJKl}^{[\lambda]}$ is defined by (A3a) and (A3b), b_J is the Jth component of the extended Burgers vector $\boldsymbol{b}$ defined as

$$b_J = u_J^- - u_J^+ = \begin{cases} u_j^- - u_j^+, & J=j=1,2,3, \\ \varphi^- - \varphi^+, & J=4, \\ \psi^- - \psi^+, & J=5, \end{cases} \tag{18}$$

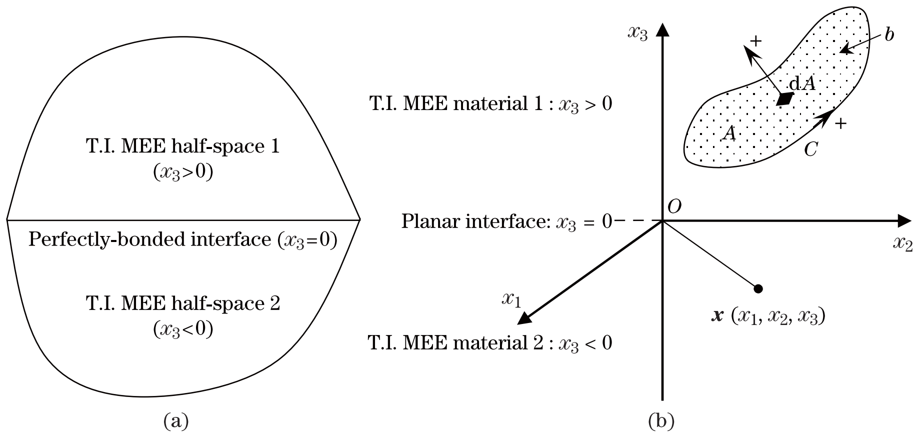

Fig. 1 Two transversely isotropic MEE half-spaces perfectly bonded together at planar interface x_3=0 and arbitrarily shaped 3D dislocation loop located in one half-space of transversely isotropic MEE bimaterial ("T.I." is abbreviation for "transversely isotropic")

in which u_J^- and u_J^+ denote the Jth component of the extended displacement at the same point on the lower and upper surface of the cut face, respectively. The positive normal of d$\boldsymbol{A}$ (see Fig. 1(b)) should point from the lower surface to the upper surface of the cut face. In this paper, we assume that the extended Burgers vector $\boldsymbol{b}$ is constant over the dislocation surface.

Substituting (1) into (17), we can obtain that

$$u_N^{[\mu][\lambda]}(\boldsymbol{x}) = \delta_{\lambda\mu} u_N^{[\lambda]}(\boldsymbol{x}) + U_N^{[\mu][\lambda]}(\boldsymbol{x}), \tag{19}$$

where

$$\begin{cases} u_N^{[\lambda]}(\boldsymbol{x}) = -\displaystyle\sum_{J,K=1}^{5}\sum_{i,l=1}^{3}\int_A \mathrm{d}A_i b_J c_{iJKl}^{[\lambda]}\frac{\partial}{\partial y_l}U_{KN}^{[\lambda]}(\boldsymbol{y};\boldsymbol{x}), \\ U_N^{[\mu][\lambda]}(\boldsymbol{x}) = -\displaystyle\sum_{J,K=1}^{5}\sum_{i,l=1}^{3}\int_A \mathrm{d}A_i b_J c_{iJKl}^{[\lambda]}\frac{\partial}{\partial y_l}U_{KN}^{[\lambda][\mu]}(\boldsymbol{y};\boldsymbol{x}). \end{cases} \tag{20}$$

The above $u_N^{[\lambda]}(\boldsymbol{x})$ denotes the Nth component of the extended displacement at point $\boldsymbol{x}\,(x_1, x_2, x_3)$ induced by the dislocation loop C in a transversely isotropic MEE full space occupied by material λ, and $U_N^{[\mu][\lambda]}(\boldsymbol{x})$ is the complementary part from the image sources due to the bimaterial interface.

Substituting (A3a), (A3b), (4), (5a), and (5b) into (20), and then making use of (15), (16), (A6), (A13), and the following Stokes' theorem[16]

$$\int_A \Big(\mathrm{d}A_i\frac{\partial}{\partial y_j} - \mathrm{d}A_j\frac{\partial}{\partial y_i}\Big)F(\boldsymbol{y}) = \sum_{k=1}^{3}\oint_C F(\boldsymbol{y})\varepsilon_{ijk}\mathrm{d}y_k,$$

or

$$\sum_{i,j,k=1}^{3}\int_A \varepsilon_{ijk}\frac{\partial}{\partial y_i}F_j(\boldsymbol{y})\mathrm{d}A_k = \sum_{l=1}^{3}\oint_C F_l(\boldsymbol{y})\mathrm{d}y_l, \tag{21}$$

we can transform the area integrals in (20) into the line-integral form as follows:

$$\begin{aligned}\begin{pmatrix} u_N^{[\lambda]}(\boldsymbol{x}) \\ U_N^{[\mu][\lambda]}(\boldsymbol{x}) \end{pmatrix} = &-\frac{b_N}{4\pi}\begin{pmatrix} \Omega_5^{[\lambda]}(\boldsymbol{x}) \\ \ell_{[\mu]}^{[\lambda]}\Omega_{N;55}^{[\lambda][\mu]}(\boldsymbol{x}) \end{pmatrix} \\ &-\frac{1}{4\pi}\sum_{J=1}^{5}\sum_{k=1}^{3}\oint_C b_J\varepsilon_{NJk}\mathrm{d}y_k\begin{pmatrix} \mathcal{U}_{N;J}^{[\lambda]}(\boldsymbol{y};\boldsymbol{x}) \\ \ell_{[\mu]}^{[\lambda]}\mathcal{U}_{N;J}^{[\lambda][\mu]}(\boldsymbol{y};\boldsymbol{x}) \end{pmatrix} \\ &-\frac{1}{4\pi}\sum_{J=1}^{5}\sum_{i,k=1}^{3}\frac{\partial}{\partial x_N}\oint_C b_J\varepsilon_{iJk}\mathrm{d}y_k\frac{\partial}{\partial y_i}\begin{pmatrix} \mathcal{U}_{N;iJ}^{[\lambda]}(\boldsymbol{y};\boldsymbol{x}) \\ \ell_{[\mu]}^{[\lambda]}\mathcal{U}_{N;iJ}^{[\lambda][\mu]}(\boldsymbol{y};\boldsymbol{x}) \end{pmatrix},\end{aligned} \tag{22}$$

where $\ell_{[\mu]}^{[\lambda]} = c_{44}^{[\lambda]}/c_{44}^{[\mu]}$,

$$\begin{cases} \Omega_5^{[\lambda]}(\boldsymbol{x}) = \displaystyle\int_A \Big(\mathrm{d}A_1\frac{\partial}{\partial y_1} + \mathrm{d}A_2\frac{\partial}{\partial y_2} + (\gamma_5^{[\lambda]})^2\mathrm{d}A_3\frac{\partial}{\partial y_3}\Big)\frac{1}{\gamma_5^{[\lambda]}R_5^{[\lambda]}}, \\ \Omega_{\beta;55}^{[\lambda][\mu]}(\boldsymbol{x}) = \displaystyle\sum_{i,k=1}^{3}\oint_C \varepsilon_{i3k}\mathrm{d}y_k\frac{\partial^2}{\partial y_i\partial y_3}\oint_C \psi_5^{[\lambda][\mu]}, \\ \Omega_{j+2;55}^{[\lambda][\mu]}(\boldsymbol{x}) = \displaystyle\sum_{i,k=1}^{3}\varepsilon_{i3k}\mathrm{d}y_k\frac{\partial^2}{\partial x_i\partial x_3}\psi_5^{[\lambda][\mu]}, \end{cases} \tag{23a}$$

$$\begin{cases} \begin{pmatrix} \mathcal{U}_{\alpha;\xi}^{[\lambda]}(\boldsymbol{y};\boldsymbol{x}) \\ \mathcal{U}_{\alpha;\xi}^{[\lambda][\mu]}(\boldsymbol{y};\boldsymbol{x}) \end{pmatrix} = \dfrac{\partial^2}{\partial y_3^2}\begin{pmatrix} \psi_5^{[\lambda]} \\ \psi_5^{[\lambda][\mu]} \end{pmatrix}, \\ \begin{pmatrix} \mathcal{U}_{\alpha;m+2}^{[\lambda]}(\boldsymbol{y};\boldsymbol{x}) \\ \mathcal{U}_{\alpha;m+2}^{[\lambda][\mu]}(\boldsymbol{y};\boldsymbol{x}) \end{pmatrix} = \dfrac{C_{m+2}^{[\lambda]}}{c_{44}^{[\lambda]}}(\gamma_5^{[\lambda]})^2\dfrac{\partial^2}{\partial y_3^2}\begin{pmatrix} \psi_5^{[\lambda]} \\ \psi_5^{[\lambda][\mu]} \end{pmatrix}, \\ \begin{pmatrix} \mathcal{U}_{i+2;\xi}^{[\lambda]}(\boldsymbol{y};\boldsymbol{x}) \\ \mathcal{U}_{i+2;\xi}^{[\lambda][\mu]}(\boldsymbol{y};\boldsymbol{x}) \end{pmatrix} = -\dfrac{\partial^2}{\partial y_3\partial x_3}\begin{pmatrix} \psi_5^{[\lambda]} \\ \psi_5^{[\lambda][\mu]} \end{pmatrix}, \\ \begin{pmatrix} \mathcal{U}_{i+2;m+2}^{[\lambda]}(\boldsymbol{y};\boldsymbol{x}) \\ \mathcal{U}_{i+2;m+2}^{[\lambda][\mu]}(\boldsymbol{y};\boldsymbol{x}) \end{pmatrix} = -\dfrac{C_{m+2}^{[\lambda]}}{c_{44}^{[\lambda]}}(\gamma_5^{[\lambda]})^2\dfrac{\partial^2}{\partial y_3\partial x_3}\begin{pmatrix} \psi_5^{[\lambda]} \\ \psi_5^{[\lambda][\mu]} \end{pmatrix}, \end{cases} \tag{23b}$$

$$\begin{cases} \begin{pmatrix} \mathcal{U}_{\alpha;\xi\eta}^{[\lambda]}(\boldsymbol{y};\boldsymbol{x}) \\ \mathcal{U}_{\alpha;\xi\eta}^{[\lambda][\mu]}(\boldsymbol{y};\boldsymbol{x}) \end{pmatrix} = 2(s_5^{[\lambda]})^2\begin{pmatrix} \psi_1^{[\lambda]} - \psi_5^{[\lambda]} \\ \psi_1^{[\lambda][\mu]} - \psi_5^{[\lambda][\mu]} \end{pmatrix}, \\ \begin{pmatrix} \mathcal{U}_{\alpha;3\eta}^{[\lambda]}(\boldsymbol{y};\boldsymbol{x}) \\ \mathcal{U}_{\alpha;3\eta}^{[\lambda][\mu]}(\boldsymbol{y};\boldsymbol{x}) \end{pmatrix} = \dfrac{1}{c_{44}^{[\lambda]}}\begin{pmatrix} c_{44}^{[\lambda]}(\psi_1^{[\lambda]} - \psi_5^{[\lambda]}) + \sum\limits_{k=1}^{3}C_{1k}^{[\lambda]}\psi_{2;k}^{[\lambda]} \\ c_{44}^{[\lambda]}(\psi_1^{[\lambda][\mu]} - \psi_5^{[\lambda][\mu]}) + \sum\limits_{k=1}^{3}C_{1k}^{[\lambda]}\psi_{2;k}^{[\lambda][\mu]} \end{pmatrix}, \\ \begin{pmatrix} \mathcal{U}_{\alpha;m(n+2)}^{[\lambda]}(\boldsymbol{y};\boldsymbol{x}) \\ \mathcal{U}_{\alpha;m(n+2)}^{[\lambda][\mu]}(\boldsymbol{y};\boldsymbol{x}) \end{pmatrix} = \dfrac{1}{c_{44}^{[\lambda]}}\begin{pmatrix} C_{n+2}^{[\lambda]}(\psi_1^{[\lambda]} - \psi_5^{[\lambda]}) + \sum\limits_{k=1}^{3}C_{nk}^{[\lambda]}\psi_{2;k}^{[\lambda]} \\ C_{n+2}^{[\lambda]}(\psi_1^{[\lambda][\mu]} - \psi_5^{[\lambda][\mu]}) + \sum\limits_{k=1}^{3}C_{nk}^{[\lambda]}\psi_{2;k}^{[\lambda][\mu]} \end{pmatrix}, \end{cases} \tag{23c}$$

and

$$\left\{\begin{aligned}
&\begin{pmatrix} \mathcal{U}^{[\lambda]}_{i+2;\xi\eta}(\boldsymbol{y};\boldsymbol{x}) \\ \\ \mathcal{U}^{[\lambda][\mu]}_{i+2;\xi\eta}(\boldsymbol{y};\boldsymbol{x}) \end{pmatrix} = 2(s^{[\lambda]}_5)^2 \begin{pmatrix} \psi^{[\lambda]}_{3;i} \\ \\ \psi^{[\lambda][\mu]}_{3;i} \end{pmatrix}, \\
&\begin{pmatrix} \mathcal{U}^{[\lambda]}_{i+2;3\eta}(\boldsymbol{y};\boldsymbol{x}) \\ \\ \mathcal{U}^{[\lambda][\mu]}_{i+2;3\eta}(\boldsymbol{y};\boldsymbol{x}) \end{pmatrix} = \frac{1}{c^{[\lambda]}_{44}} \begin{pmatrix} c^{[\lambda]}_{44}\psi^{[\lambda]}_{3;i} + c^{[\lambda]}_{44}\psi^{[\lambda]}_{5} + \sum\limits_{k=1}^{3} C^{[\lambda]}_{1k}\psi^{[\lambda]}_{4;ki} \\ \\ c^{[\lambda]}_{44}\psi^{[\lambda][\mu]}_{3;i} + c^{[\lambda]}_{44}\psi^{[\lambda][\mu]}_{5} + \sum\limits_{k=1}^{3} C^{[\lambda]}_{1k}\psi^{[\lambda][\mu]}_{4;ki} \end{pmatrix}, \\
&\begin{pmatrix} \mathcal{U}^{[\lambda]}_{i+2;m(n+2)}(\boldsymbol{y};\boldsymbol{x}) \\ \\ \mathcal{U}^{[\lambda][\mu]}_{i+2;m(n+2)}(\boldsymbol{y};\boldsymbol{x}) \end{pmatrix} = \frac{1}{c^{[\lambda]}_{44}} \begin{pmatrix} C^{[\lambda]}_{n+2}\psi^{[\lambda]}_{3;i} + \delta_{in}c^{[\lambda]}_{44}\psi^{[\lambda]}_{5} + \sum\limits_{k=1}^{3} C^{[\lambda]}_{nk}\psi^{[\lambda]}_{4;ki} \\ \\ C^{[\lambda]}_{n+2}\psi^{[\lambda][\mu]}_{3;i} + \delta_{in}c^{[\lambda]}_{44}\psi^{[\lambda][\mu]}_{5} + \sum\limits_{k=1}^{3} C^{[\lambda]}_{nk}\psi^{[\lambda][\mu]}_{4;ki} \end{pmatrix},
\end{aligned}\right. \tag{23d}$$

in which the material constants $C^{[\lambda]}_{ij}$ and $C^{[\lambda]}_{J}$ are defined in (A12a) and (A12b), respectively. It can be observed from (23c) and (23d) that

$$\begin{pmatrix} \mathcal{U}^{[\lambda]}_{i;mn}(\boldsymbol{y};\boldsymbol{x}) \\ \\ \mathcal{U}^{[\lambda][\mu]}_{i;mn}(\boldsymbol{y};\boldsymbol{x}) \end{pmatrix} = \begin{pmatrix} \mathcal{U}^{[\lambda]}_{i;nm}(\boldsymbol{y};\boldsymbol{x}) \\ \\ \mathcal{U}^{[\lambda][\mu]}_{i;nm}(\boldsymbol{y};\boldsymbol{x}) \end{pmatrix}. \tag{24}$$

Note that the area integral $\Omega^{[\lambda]}_5(\boldsymbol{x})$ in (23a) denotes the quasi solid angle subtended by the cut face A of the dislocation loop C in material λ at point $\boldsymbol{x}$, which can also be transformed into a line integral[17].

3.2 Extended stresses of arbitrarily shaped 3D dislocation loop

Using the constitutive relation for transversely isotropic MEE materials as shown in (A1b), we can derive from (19) the extended stresses as follows:

$$\sigma^{[\mu][\lambda]}_{iJ}(\boldsymbol{x}) = \delta_{\lambda\mu}\sigma^{[\lambda]}_{iJ}(\boldsymbol{x}) + S^{[\mu][\lambda]}_{iJ}(\boldsymbol{x}), \tag{25}$$

in which

$$\left\{\begin{aligned}
&\sigma^{[\lambda]}_{iJ}(\boldsymbol{x}) = \sum_{K=1}^{5}\sum_{l=1}^{3} c^{[\lambda]}_{iJKl}\frac{\partial}{\partial x_l}u^{[\lambda]}_K(\boldsymbol{x}), \\
&S^{[\mu][\lambda]}_{iJ}(\boldsymbol{x}) = \sum_{K=1}^{5}\sum_{l=1}^{3} c^{[\mu]}_{iJKl}\frac{\partial}{\partial x_l}U^{[\mu][\lambda]}_K(\boldsymbol{x}),
\end{aligned}\right. \tag{26}$$

where $\sigma^{[\mu][\lambda]}_{iJ}(\boldsymbol{x})$ denotes the extended stress at point $\boldsymbol{x}\,(x_1,\ x_2,\ x_3)$ in transversely isotropic MEE material μ due to an arbitrarily shaped 3D dislocation loop C located in transversely isotropic MEE material λ, $\sigma^{[\lambda]}_{iJ}(\boldsymbol{x})$ is the extended stresses at point $\boldsymbol{x}\,(x_1,\ x_2,\ x_3)$ induced by the same dislocation loop C in a transversely isotropic MEE full space occupied by material λ, $S^{[\mu][\lambda]}_{iJ}(\boldsymbol{x})$ is the complementary part from the image sources due to the bimaterial interface.

Substituting (22) into (26), we can express $\sigma^{[\lambda]}_{iJ}(\boldsymbol{x})$ and $S^{[\mu][\lambda]}_{iJ}(\boldsymbol{x})$ in terms of line integrals as

$$\begin{aligned}\begin{pmatrix} \sigma_{pQ}^{[\lambda]}(\boldsymbol{x}) \\ S_{pQ}^{[\mu][\lambda]}(\boldsymbol{x}) \end{pmatrix} = &-\frac{1}{4\pi}\sum_{J=1}^{5}\sum_{i=1}^{3}\oint_C b_J(\varepsilon_{iJp}\mathrm{d}y_Q+\varepsilon_{iJQ}\mathrm{d}y_p)\frac{\partial}{\partial y_i}\begin{pmatrix} C_Q^{[\lambda]}\mathcal{S}_{pQ;J}^{[\lambda]}(\boldsymbol{y};\boldsymbol{x}) \\ \ell_{[\mu]}^{[\lambda]}C_Q^{[\mu]}\mathcal{S}_{pQ;J}^{[\lambda][\mu]}(\boldsymbol{y};\boldsymbol{x}) \end{pmatrix} \\ &-\frac{1}{4\pi}\sum_{J=1}^{5}\sum_{i,k=1}^{3}\oint_C b_J\varepsilon_{iJk}\mathrm{d}y_k\frac{\partial}{\partial y_i}\frac{\partial^2}{\partial x_p\partial x_Q}\begin{pmatrix} C_Q^{[\lambda]}\mathcal{S}_{pQ;iJ}^{[\lambda]}(\boldsymbol{y};\boldsymbol{x}) \\ \ell_{[\mu]}^{[\lambda]}C_Q^{[\mu]}\mathcal{S}_{pQ;iJ}^{[\lambda][\mu]}(\boldsymbol{y};\boldsymbol{x}) \end{pmatrix} \\ &+\frac{\delta_{pQ}}{4\pi}\sum_{J=1}^{5}\sum_{i,k=1}^{3}\oint_C b_J\varepsilon_{iJk}\mathrm{d}y_k\frac{\partial}{\partial y_i}\Big(\frac{\partial^2}{\partial x_1^2}+\frac{\partial^2}{\partial x_2^2}\Big)\begin{pmatrix} C_Q^{[\lambda]}\mathcal{S}_{pQ;iJ}^{[\lambda]}(\boldsymbol{y};\boldsymbol{x}) \\ \ell_{[\mu]}^{[\lambda]}C_Q^{[\mu]}\mathcal{S}_{pQ;iJ}^{[\lambda][\mu]}(\boldsymbol{y};\boldsymbol{x}) \end{pmatrix} \\ &+\frac{\delta_{pQ}}{4\pi}\sum_{J=1}^{5}\sum_{i,k=1}^{3}\oint_C b_J\varepsilon_{iJk}\mathrm{d}y_k\frac{\partial}{\partial y_i}\frac{\partial^2}{\partial x_3^2}\begin{pmatrix} C_Q^{[\lambda]}\mathcal{S}_{3Q;iJ}^{[\lambda]}(\boldsymbol{y};\boldsymbol{x}) \\ \ell_{[\mu]}^{[\lambda]}C_Q^{[\mu]}\mathcal{S}_{3Q;iJ}^{[\lambda][\mu]}(\boldsymbol{y};\boldsymbol{x}) \end{pmatrix}, \end{aligned} \tag{27}$$

where

$$\begin{cases} \begin{pmatrix} \mathcal{S}_{\alpha\beta;N}^{[\lambda]}(\boldsymbol{y};\boldsymbol{x}) \\ \mathcal{S}_{\alpha\beta;N}^{[\lambda][\mu]}(\boldsymbol{y};\boldsymbol{x}) \end{pmatrix} = \dfrac{C_N^{[\lambda]}}{c_{44}^{[\lambda]}}\dfrac{\partial^2}{\partial x_3^2}\begin{pmatrix} \psi_5^{[\lambda]} \\ \psi_5^{[\lambda][\mu]} \end{pmatrix}, \\ \begin{pmatrix} \mathcal{S}_{\alpha(j+2);N}^{[\lambda]}(\boldsymbol{y};\boldsymbol{x}) \\ \mathcal{S}_{\alpha(j+2);N}^{[\lambda][\mu]}(\boldsymbol{y};\boldsymbol{x}) \end{pmatrix} = -\dfrac{C_N^{[\lambda]}}{c_{44}^{[\lambda]}}\dfrac{\partial^2}{\partial x_3\partial y_3}\begin{pmatrix} \psi_5^{[\lambda]} \\ \psi_5^{[\lambda][\mu]} \end{pmatrix}, \\ \begin{pmatrix} \mathcal{S}_{3\beta;N}^{[\lambda]}(\boldsymbol{y};\boldsymbol{x}) \\ \mathcal{S}_{3\beta;N}^{[\lambda][\mu]}(\boldsymbol{y};\boldsymbol{x}) \end{pmatrix} = \begin{pmatrix} \mathcal{S}_{\beta3;N}^{[\lambda]}(\boldsymbol{y};\boldsymbol{x}) \\ \mathcal{S}_{\beta3;N}^{[\lambda][\mu]}(\boldsymbol{y};\boldsymbol{x}) \end{pmatrix}, \\ \begin{pmatrix} \mathcal{S}_{3(j+2);N}^{[\lambda]}(\boldsymbol{y};\boldsymbol{x}) \\ \mathcal{S}_{3(j+2);N}^{[\lambda][\mu]}(\boldsymbol{y};\boldsymbol{x}) \end{pmatrix} = \dfrac{C_N^{[\lambda]}}{c_{44}^{[\lambda]}}\dfrac{\partial^2}{\partial y_3^2}\begin{pmatrix} \psi_5^{[\lambda]} \\ \psi_5^{[\lambda][\mu]} \end{pmatrix}, \end{cases} \tag{28a}$$

$$\begin{cases} \begin{pmatrix} \mathcal{S}_{\alpha\beta;\xi\eta}^{[\lambda]}(\boldsymbol{y};\boldsymbol{x}) \\ \mathcal{S}_{\alpha\beta;\xi\eta}^{[\lambda][\mu]}(\boldsymbol{y};\boldsymbol{x}) \end{pmatrix} = 2(s_5^{[\lambda]})^2\begin{pmatrix} 2(s_5^{[\lambda]})^2(\psi_1^{[\lambda]}-\psi_5^{[\lambda]}) \\ 2(s_5^{[\mu]})^2(\psi_1^{[\lambda][\mu]}-\psi_5^{[\lambda][\mu]}) \end{pmatrix}, \\ \begin{pmatrix} \mathcal{S}_{\alpha\beta;\xi(n+2)}^{[\lambda]}(\boldsymbol{y};\boldsymbol{x}) \\ \mathcal{S}_{\alpha\beta;\xi(n+2)}^{[\lambda][\mu]}(\boldsymbol{y};\boldsymbol{x}) \end{pmatrix} \\ = \dfrac{1}{c_{44}^{[\lambda]}}\begin{pmatrix} 2(s_5^{[\lambda]})^2\Big(C_{n+2}^{[\lambda]}(\psi_1^{[\lambda]}-\psi_5^{[\lambda]})+\sum\limits_{q=1}^{3}C_{nq}^{[\lambda]}\psi_{2;q}^{[\lambda]}\Big) \\ 2(s_5^{[\mu]})^2\Big(C_{n+2}^{[\lambda]}(\psi_1^{[\lambda][\mu]}-\psi_5^{[\lambda][\mu]})+\sum\limits_{q=1}^{3}C_{nq}^{[\lambda]}\psi_{2;q}^{[\lambda][\mu]}\Big) \end{pmatrix}, \\ \begin{pmatrix} \mathcal{S}_{\alpha\beta;3N}^{[\lambda]}(\boldsymbol{y};\boldsymbol{x}) \\ \mathcal{S}_{\alpha\beta;3N}^{[\lambda][\mu]}(\boldsymbol{y};\boldsymbol{x}) \end{pmatrix} = \dfrac{1}{c_{44}^{[\lambda]}}\begin{pmatrix} 2(s_5^{[\lambda]})^2\Big(c_{44}^{[\lambda]}(\psi_1^{[\lambda]}-\psi_5^{[\lambda]})+\sum\limits_{q=1}^{3}C_{1q}^{[\lambda]}\psi_{2;q}^{[\lambda]}\Big) \\ 2(s_5^{[\mu]})^2\Big(c_{44}^{[\lambda]}(\psi_1^{[\lambda][\mu]}-\psi_5^{[\lambda][\mu]})+\sum\limits_{q=1}^{3}C_{1q}^{[\lambda]}\psi_{2;q}^{[\lambda][\mu]}\Big) \end{pmatrix}, \end{cases} \tag{28b}$$

and

$$\left\{\begin{array}{l}
\begin{pmatrix} C^{[\lambda]}_{j+2}\mathcal{S}^{[\lambda]}_{i(j+2);\xi\eta}(\boldsymbol{y};\boldsymbol{x}) \\ C^{[\mu]}_{j+2}\mathcal{S}^{[\lambda][\mu]}_{i(j+2);\xi\eta}(\boldsymbol{y};\boldsymbol{x}) \end{pmatrix} = 2(s^{[\lambda]}_5)^2 \begin{pmatrix} C^{[\lambda]}_{j+2}(\psi^{[\lambda]}_1 - \psi^{[\lambda]}_5) + \sum\limits_{q=1}^{3} C^{[\lambda]}_{jq}\psi^{[\lambda]}_{3;q} \\ C^{[\mu]}_{j+2}(\psi^{[\lambda][\mu]}_1 - \psi^{[\lambda][\mu]}_5) + \sum\limits_{q=1}^{3} C^{[\mu]}_{jq}\psi^{[\lambda][\mu]}_{3;q} \end{pmatrix}, \\
\begin{pmatrix} C^{[\lambda]}_{j+2}\mathcal{S}^{[\lambda]}_{i(j+2);\xi(n+2)}(\boldsymbol{y};\boldsymbol{x}) \\ C^{[\mu]}_{j+2}\mathcal{S}^{[\lambda][\mu]}_{i(j+2);\xi(n+2)}(\boldsymbol{y};\boldsymbol{x}) \end{pmatrix} = \dfrac{1}{c^{[\lambda]}_{44}} \\
\cdot \begin{pmatrix} C^{[\lambda]}_{j+2}\left(C^{[\lambda]}_{n+2}\psi^{[\lambda]}_1 + \sum\limits_{q=1}^{3} C^{[\lambda]}_{nq}\psi^{[\lambda]}_{2;q}\right) + \sum\limits_{q=1}^{3} C^{[\lambda]}_{jq}\left(C^{[\lambda]}_{n+2}\psi^{[\lambda]}_{3;q} + \sum\limits_{p=1}^{3} C^{[\lambda]}_{np}\psi^{[\lambda]}_{4;pq}\right) \\ C^{[\mu]}_{j+2}\left(C^{[\lambda]}_{n+2}\psi^{[\lambda][\mu]}_1 + \sum\limits_{q=1}^{3} C^{[\lambda]}_{nq}\psi^{[\lambda][\mu]}_{2;q}\right) + \sum\limits_{q=1}^{3} C^{[\mu]}_{jq}\left(C^{[\lambda]}_{n+2}\psi^{[\lambda][\mu]}_{3;q} + \sum\limits_{p=1}^{3} C^{[\lambda]}_{np}\psi^{[\lambda][\mu]}_{4;pq}\right) \end{pmatrix}, \\
\begin{pmatrix} C^{[\lambda]}_{j+2}\mathcal{S}^{[\lambda]}_{i(j+2);3N}(\boldsymbol{y};\mathrm{x}) \\ C^{[\mu]}_{j+2}\mathcal{S}^{[\lambda][\mu]}_{i(j+2);3N}(\boldsymbol{y};\boldsymbol{x}) \end{pmatrix} = \dfrac{1}{c^{[\lambda]}_{44}} \\
\cdot \begin{pmatrix} C^{[\lambda]}_{j+2}\left(c^{[\lambda]}_{44}\psi^{[\lambda]}_1 + \sum\limits_{q=1}^{3} C^{[\lambda]}_{1q}\psi^{[\lambda]}_{2;q}\right) + \sum\limits_{q=1}^{3} C^{[\lambda]}_{jq}\left(c^{[\lambda]}_{44}\psi^{[\lambda]}_{3;q} + \sum\limits_{p=1}^{3} C^{[\lambda]}_{1p}\psi^{[\lambda]}_{4;pq}\right) \\ C^{[\mu]}_{j+2}\left(c^{[\lambda]}_{44}\psi^{[\lambda][\mu]}_1 + \sum\limits_{q=1}^{3} C^{[\lambda]}_{1q}\psi^{[\lambda][\mu]}_{2;q}\right) + \sum\limits_{q=1}^{3} C^{[\mu]}_{jq}\left(c^{[\lambda]}_{44}\psi^{[\lambda][\mu]}_{3;q} + \sum\limits_{p=1}^{3} C^{[\lambda]}_{1p}\psi^{[\lambda][\mu]}_{4;pq}\right) \end{pmatrix}, \\
\begin{pmatrix} \mathcal{S}^{[\lambda]}_{3\beta;mN}(\boldsymbol{y};\boldsymbol{x}) \\ \mathcal{S}^{[\lambda][\mu]}_{3\beta;mN}(\boldsymbol{y};\boldsymbol{x}) \end{pmatrix} = \begin{pmatrix} \mathcal{S}^{[\lambda]}_{\beta 3;mN}(\boldsymbol{y};\boldsymbol{x}) \\ \mathcal{S}^{[\lambda][\mu]}_{\beta 3;mN}(\boldsymbol{y};\boldsymbol{x}) \end{pmatrix}.
\end{array}\right. \tag{28c}$$

During the derivation of (27), we have made use of (15) and (16), along with the following relations:

$$\delta_{\alpha\xi}\varepsilon_{\beta\eta 3} - \delta_{\alpha\eta}\varepsilon_{\beta\xi 3} = \delta_{\alpha\beta}\varepsilon_{\xi\eta 3}, \tag{29}$$

and

$$\begin{aligned} &\sum_{\tau=1}^{2}\oint_C \varepsilon_{\alpha 3\tau}\mathrm{d}y_\tau \frac{\partial^2}{\partial y_\alpha \partial y_\xi}\begin{pmatrix} \psi^{[\lambda]}_5 \\ \psi^{[\lambda][\mu]}_5 \end{pmatrix} \\ &= \oint_C \varepsilon_{\alpha\xi 3}\mathrm{d}y_3 \frac{\partial^2}{\partial y_\alpha \partial y_3}\begin{pmatrix} \psi^{[\lambda]}_5 \\ \psi^{[\lambda][\mu]}_5 \end{pmatrix} + \sum_{\tau=1}^{2}\oint_C \varepsilon_{\xi 3\tau}\mathrm{d}y_\tau \frac{\partial^2}{\partial y_\alpha \partial y_\alpha}\begin{pmatrix} \psi^{[\lambda]}_5 \\ \psi^{[\lambda][\mu]}_5 \end{pmatrix}. \end{aligned} \tag{30}$$

(30) can be verified by Stokes' theorem in (21).

By virtue of (9), we can obtain from (28b) and (28c) that

$$\begin{pmatrix} \mathcal{S}^{[\lambda]}_{pq;iJ}(\boldsymbol{y};\boldsymbol{x}) \\ \mathcal{S}^{[\lambda][\mu]}_{pq;iJ}(\boldsymbol{y};\boldsymbol{x}) \end{pmatrix} = \begin{pmatrix} \mathcal{S}^{[\lambda]}_{qp;iJ}(\boldsymbol{y};\boldsymbol{x}) \\ \mathcal{S}^{[\lambda][\mu]}_{qp;iJ}(\boldsymbol{y};\boldsymbol{x}) \end{pmatrix}, \quad \begin{pmatrix} \mathcal{S}^{[\lambda]}_{pQ;ij}(\boldsymbol{y};\boldsymbol{x}) \\ \mathcal{S}^{[\lambda][\mu]}_{pQ;ij}(\boldsymbol{y};\boldsymbol{x}) \end{pmatrix} = \begin{pmatrix} \mathcal{S}^{[\lambda]}_{pQ;ji}(\boldsymbol{y};\boldsymbol{x}) \\ \mathcal{S}^{[\lambda][\mu]}_{pQ;ji}(\boldsymbol{y};\boldsymbol{x}) \end{pmatrix}, \tag{31a}$$

and

$$c^{[\lambda]}_{44}\mathcal{S}^{[\lambda]}_{\xi q;\alpha J}(\boldsymbol{y};\boldsymbol{x}) = C^{[\lambda]}_J \mathcal{S}^{[\lambda]}_{\alpha J;\xi q}(\boldsymbol{y};\boldsymbol{x}). \tag{31b}$$

3.3 Interaction energy between two arbitrarily shaped 3D dislocation loops

Suppose that there are two arbitrarily shaped 3D dislocation loops C and $\widetilde{C}$ in transversely isotropic MEE bimaterials. The dislocation loop C is located in material λ and bounds a curved surface A with an extended Burgers vector $\boldsymbol{b}$, the dislocation loop $\widetilde{C}$ is located in material μ and bounds a curved surface $\widetilde{A}$ with an extended Burgers vector $\widetilde{\boldsymbol{b}}$. Based upon the classical theory of dislocations[15], the interaction energy $w_{\mathrm{I}}^{[\mu][\lambda]}$ between the two dislocation loops can be expressed as

$$w_{\mathrm{I}}^{[\mu][\lambda]} = \delta_{\lambda\mu} w_{\mathrm{I}}^{[\lambda]} + W_{\mathrm{I}}^{[\mu][\lambda]}, \tag{32}$$

in which

$$w_{\mathrm{I}}^{[\lambda]} = \sum_{Q=1}^{5}\sum_{p=1}^{3}\int_{\widetilde{A}} \mathrm{d}\widetilde{A}_p \widetilde{b}_Q \sigma_{pQ}^{[\lambda]}(\boldsymbol{x}) \ , \ \ W_{\mathrm{I}}^{[\mu][\lambda]} = \sum_{Q=1}^{5}\sum_{p=1}^{3}\int_{\widetilde{A}} \mathrm{d}\widetilde{A}_p \widetilde{b}_Q S_{pQ}^{[\mu][\lambda]}(\boldsymbol{x}), \tag{33}$$

where $\sigma_{pQ}^{[\lambda]}(\boldsymbol{x})$ and $S_{pQ}^{[\mu][\lambda]}(\boldsymbol{x})$ are the two parts of the extended stress induced by the dislocation loop C, as given in (27), $\mathrm{d}\widetilde{A}_p$ is the pth component of the vector area element $\mathrm{d}\widetilde{\boldsymbol{A}}$ defined at point $\boldsymbol{x}\,(x_1, x_2, x_3)$ on the dislocation surface $\widetilde{A}$. The above $w_{\mathrm{I}}^{[\lambda]}$ is the interaction energy between the two dislocation loops $\widetilde{C}$ and C in a transversely isotropic MEE full space occupied by material λ, and $W_{\mathrm{I}}^{[\mu][\lambda]}$ is the complementary part from the image sources due to the bimaterial interface.

Substituting (27) into (33), and then making use of (16), the Stokes theorem in (21) and the following relations:

$$\varepsilon_{\alpha\beta 3}\varepsilon_{\xi\eta 3} = \delta_{\alpha\xi}\delta_{\beta\eta} - \delta_{\alpha\eta}\delta_{\beta\xi}, \quad \sum_{\beta=1}^{2}\varepsilon_{\alpha\beta 3}\varepsilon_{\xi\beta 3} = \delta_{\alpha\xi}, \tag{34}$$

$$\sum_{i=1}^{3}\oint_C \mathrm{d}y_i \frac{\partial}{\partial y_i}\frac{\partial^2}{\partial y_3^2}\begin{pmatrix} \psi_5^{[\lambda]} \\ \psi_5^{[\lambda][\mu]} \end{pmatrix} = \oint_C \mathrm{d}\frac{\partial^2}{\partial y_3^2}\begin{pmatrix} \psi_5^{[\lambda]} \\ \psi_5^{[\lambda][\mu]} \end{pmatrix} = \begin{pmatrix} 0 \\ 0 \end{pmatrix}, \tag{35}$$

we can thus express the interaction energy in terms of double line integrals as

$$\begin{aligned}\begin{pmatrix} w_{\mathrm{I}}^{[\lambda]} \\ W_{\mathrm{I}}^{[\mu][\lambda]} \end{pmatrix} = &-\frac{1}{2\pi}\sum_{I,J=1}^{5}\sum_{k,p,q=1}^{3}\widetilde{b}_I b_J \oint_{\widetilde{C}}\mathrm{d}x_p\oint_C \mathrm{d}y_q \varepsilon_{IJk}\varepsilon_{pqk}\begin{pmatrix} C_I^{[\lambda]}\mathcal{W}_{Jq}^{[\lambda]}(\boldsymbol{y};\boldsymbol{x}) \\ \ell_{[\mu]}^{[\lambda]} C_I^{[\mu]}\mathcal{W}_{Jq}^{[\lambda][\mu]}(\boldsymbol{y};\boldsymbol{x}) \end{pmatrix} \\ &+\frac{1}{4\pi}\sum_{I,J=1}^{5}\widetilde{b}_I b_J \oint_{\widetilde{C}}\mathrm{d}x_I\oint_C \mathrm{d}y_J\begin{pmatrix} C_I^{[\lambda]}\mathcal{W}_J^{[\lambda]}(\boldsymbol{y};\boldsymbol{x}) \\ \ell_{[\mu]}^{[\lambda]} C_I^{[\mu]}\mathcal{W}_J^{[\lambda][\mu]}(\boldsymbol{y};\boldsymbol{x}) \end{pmatrix} \\ &-\frac{1}{4\pi}\sum_{I,J=1}^{5}\sum_{m,n,p,q=1}^{3}\widetilde{b}_I b_J \oint_{\widetilde{C}}\mathrm{d}x_m\oint_C \mathrm{d}y_n \varepsilon_{pIm}\varepsilon_{qJn} \\ &\cdot\frac{\partial^2}{\partial x_p \partial y_q}\begin{pmatrix} C_I^{[\lambda]}\mathcal{S}_{pI;qJ}^{[\lambda]}(\boldsymbol{y};\boldsymbol{x}) \\ \ell_{[\mu]}^{[\lambda]} C_I^{[\mu]}\mathcal{S}_{pI;qJ}^{[\lambda][\mu]}(\boldsymbol{y};\boldsymbol{x}) \end{pmatrix},\end{aligned} \tag{36}$$

in which

$$\begin{cases} \begin{pmatrix} \mathcal{W}^{[\lambda]}_{\alpha\beta}(\boldsymbol{y};\boldsymbol{x}) \\ \mathcal{W}^{[\lambda][\mu]}_{\alpha\beta}(\boldsymbol{y};\boldsymbol{x}) \end{pmatrix} = -\dfrac{\partial^2}{\partial x_3 \partial y_3} \begin{pmatrix} \psi_5^{[\lambda]} \\ \psi_5^{[\lambda][\mu]} \end{pmatrix}, \\[2ex] \begin{pmatrix} \mathcal{W}^{[\lambda]}_{(i+2)\beta}(\boldsymbol{y};\boldsymbol{x}) \\ \mathcal{W}^{[\lambda][\mu]}_{(i+2)\beta}(\boldsymbol{y};\boldsymbol{x}) \end{pmatrix} = \dfrac{C^{[\lambda]}_{i+2}}{c^{[\lambda]}_{44}} \dfrac{\partial^2}{\partial x_3^2} \begin{pmatrix} \psi_5^{[\lambda]} \\ \psi_5^{[\lambda][\mu]} \end{pmatrix}, \\[2ex] \begin{pmatrix} \mathcal{W}^{[\lambda]}_{\alpha 3}(\boldsymbol{y};\boldsymbol{x}) \\ \mathcal{W}^{[\lambda][\mu]}_{\alpha 3}(\boldsymbol{y};\boldsymbol{x}) \end{pmatrix} = \dfrac{\partial^2}{\partial y_3^2} \begin{pmatrix} \psi_5^{[\lambda]} \\ \psi_5^{[\lambda][\mu]} \end{pmatrix}, \\[2ex] \begin{pmatrix} \mathcal{W}^{[\lambda]}_{(i+2)3}(\boldsymbol{y};\boldsymbol{x}) \\ \mathcal{W}^{[\lambda][\mu]}_{(i+2)3}(\boldsymbol{y};\boldsymbol{x}) \end{pmatrix} = -\dfrac{C^{[\lambda]}_{i+2}}{c^{[\lambda]}_{44}} \dfrac{\partial^2}{\partial x_3 \partial y_3} \begin{pmatrix} \psi_5^{[\lambda]} \\ \psi_5^{[\lambda][\mu]} \end{pmatrix}, \end{cases} \tag{37a}$$

and

$$\begin{cases} \begin{pmatrix} \mathcal{W}^{[\lambda]}_{\alpha}(\boldsymbol{y};\boldsymbol{x}) \\ \mathcal{W}^{[\lambda][\mu]}_{\alpha}(\boldsymbol{y};\boldsymbol{x}) \end{pmatrix} = -\dfrac{\partial^2}{\partial x_3 \partial y_3} \begin{pmatrix} \psi_5^{[\lambda]} \\ \psi_5^{[\lambda][\mu]} \end{pmatrix}, \\[2ex] \begin{pmatrix} \mathcal{W}^{[\lambda]}_{i+2}(\boldsymbol{y};\boldsymbol{x}) \\ \mathcal{W}^{[\lambda][\mu]}_{i+2}(\boldsymbol{y};\boldsymbol{x}) \end{pmatrix} = -\dfrac{C^{[\lambda]}_{i+2}}{c^{[\lambda]}_{44}} \dfrac{\partial^2}{\partial x_3 \partial y_3} \begin{pmatrix} \psi_5^{[\lambda]} \\ \psi_5^{[\lambda][\mu]} \end{pmatrix}. \end{cases} \tag{37b}$$

As an immediate application of (36), we now consider one dislocation loop C with an extended Burgers vector (b_1,b_2,b_3,0,0) and another dislocation loop $\tilde{C}$ with an extended Burgers vector $(\tilde{b}_1, \tilde{b}_2, \tilde{b}_3, 0, 0)$, both of which are located in the transversely isotropic MEE full space occupied by material λ. In this special case, the interaction energy between the two dislocation loops can be expressed in an elegant way as

$$\begin{aligned} w_{\mathrm{I}}^{[\lambda]} = &-\frac{c^{[\lambda]}_{44}}{4\pi} \sum_{i,j=1}^{3} \oint_{\tilde{C}} \mathrm{d}x_i \oint_{C} \mathrm{d}y_j \tilde{b}_i b_j \frac{\partial^2}{\partial y_3^2} \psi_5^{[\lambda]} \\ &- \frac{c^{[\lambda]}_{44}}{4\pi} \sum_{i,j=1}^{3} \oint_{\tilde{C}} \mathrm{d}x_j \oint_{C} \mathrm{d}y_i \tilde{b}_i b_j \left(-2 \frac{\partial^2}{\partial y_3^2} \psi_5^{[\lambda]} + \sum_{k=1}^{3} \frac{\partial^2}{\partial y_k^2} \mathcal{S}^{[\lambda]}_{13;1k}(\boldsymbol{y};\boldsymbol{x}) \right) \\ &- \frac{c^{[\lambda]}_{44}}{4\pi} \sum_{i,j,k=1}^{3} \oint_{\tilde{C}} \mathrm{d}x_k \oint_{C} \mathrm{d}y_k \left(\tilde{b}_i b_j \frac{\partial^2}{\partial y_i \partial y_j} - \tilde{b}_i b_i \frac{\partial^2}{\partial y_j \partial y_j} \right) \mathcal{W}^{[\lambda]}_{ij;k}(\boldsymbol{y};\boldsymbol{x}), \end{aligned} \tag{38}$$

in which

$$\begin{cases} \mathcal{W}^{[\lambda]}_{ij;\xi}(\boldsymbol{y};\boldsymbol{x}) = \mathcal{S}^{[\lambda]}_{ij;\xi 3}(\boldsymbol{y};\boldsymbol{x}), \\ \mathcal{W}^{[\lambda]}_{ij;3}(\boldsymbol{y};\boldsymbol{x}) = \mathcal{S}^{[\lambda]}_{ij;11}(\boldsymbol{y};\boldsymbol{x}). \end{cases} \tag{39}$$

During the derivation of (38) from (36), we have made use of (16) and (34), along with the following relations:

$$\begin{cases} \displaystyle\sum_{\tau=1}^{2} \oint_{\widetilde{C}} \varepsilon_{\alpha 3\tau} \mathrm{d}x_\tau \frac{\partial^2}{\partial x_\alpha \partial x_\xi} \mathcal{S}^{[\lambda]}_{\beta\gamma;\eta 3}(\boldsymbol{y};\boldsymbol{x}) \\ \displaystyle = \oint_{\widetilde{C}} \varepsilon_{\alpha\xi 3} \mathrm{d}x_3 \frac{\partial^2}{\partial x_\alpha \partial x_3} \mathcal{S}^{[\lambda]}_{\beta\gamma;\eta 3}(\boldsymbol{y};\boldsymbol{x}) + \sum_{\tau=1}^{2} \oint_{\widetilde{C}} \varepsilon_{\xi 3\tau} \mathrm{d}x_\tau \frac{\partial^2}{\partial x_\alpha \partial x_\alpha} \mathcal{S}^{[\lambda]}_{\beta\gamma;\eta 3}(\boldsymbol{y};\boldsymbol{x}), \\ \displaystyle\sum_{\tau=1}^{2} \oint_{C} \varepsilon_{\alpha 3\tau} \mathrm{d}y_\tau \frac{\partial^2}{\partial y_\alpha \partial y_\xi} \mathcal{S}^{[\lambda]}_{\beta\gamma;\eta 3}(\boldsymbol{y};\boldsymbol{x}) \\ \displaystyle = \oint_{C} \varepsilon_{\alpha\xi 3} \mathrm{d}y_3 \frac{\partial^2}{\partial y_\alpha \partial y_3} \mathcal{S}^{[\lambda]}_{\beta\gamma;\eta 3}(\boldsymbol{y};\boldsymbol{x}) + \sum_{\tau=1}^{2} \oint_{C} \varepsilon_{\xi 3\tau} \mathrm{d}y_\tau \frac{\partial^2}{\partial y_\alpha \partial y_\alpha} \mathcal{S}^{[\lambda]}_{\beta\gamma;\eta 3}(\boldsymbol{y};\boldsymbol{x}), \end{cases} \tag{40}$$

and

$$\begin{cases} \displaystyle\sum_{i=1}^{3} \oint_{\widetilde{C}} \mathrm{d}x_i \frac{\partial}{\partial x_i} \frac{\partial}{\partial x_n} \mathcal{S}^{[\lambda]}_{\alpha j;\xi 3}(\boldsymbol{y};\boldsymbol{x}) = \oint_{\widetilde{C}} \mathrm{d} \frac{\partial}{\partial x_n} \mathcal{S}^{[\lambda]}_{\alpha j;\xi 3}(\boldsymbol{y};\boldsymbol{x}) = 0, \\ \displaystyle\sum_{i=1}^{3} \oint_{C} \mathrm{d}y_i \frac{\partial}{\partial y_i} \frac{\partial}{\partial y_n} \mathcal{S}^{[\lambda]}_{\alpha j;\xi 3}(\boldsymbol{y};\boldsymbol{x}) = \oint_{C} \mathrm{d} \frac{\partial}{\partial y_n} \mathcal{S}^{[\lambda]}_{\alpha j;\xi 3}(\boldsymbol{y};\boldsymbol{x}) = 0. \end{cases} \tag{41}$$

(40) can be verified by Stokes' theorem in (21).

Now, we consider a single dislocation loop C with an extended Burgers vector $\boldsymbol{b}$, which bounds a curved surface A in material λ of the transversely isotropic MEE bimaterial. According to Hirth and Lothe[15], we can express the self-energy $w_{\mathrm{S}}^{[\lambda]}$ of the dislocation loop C as

$$w_{\mathrm{S}}^{[\lambda]} = w_{\mathrm{FS}}^{[\lambda]} + W_{\mathrm{IS}}^{[\lambda]}, \tag{42}$$

where

$$w_{\mathrm{FS}}^{[\lambda]} = \frac{1}{2} \sum_{Q=1}^{5} \sum_{p=1}^{3} \int_A \mathrm{d}A_p b_Q \sigma_{pQ}^{[\lambda]}(\boldsymbol{x}) \ , \ \ W_{\mathrm{IS}}^{[\lambda]} = \frac{1}{2} \sum_{Q=1}^{5} \sum_{p=1}^{3} \int_A \mathrm{d}A_p b_Q S_{pQ}^{[\mu][\lambda]}(\boldsymbol{x}), \tag{43}$$

in which $\sigma_{pQ}^{[\lambda]}(\boldsymbol{x})$ and $S_{pQ}^{[\mu][\lambda]}(\boldsymbol{x})$ are the two parts of the extended stress induced by the dislocation loop C, as given in (27); $\mathrm{d}A_p$ is the pth component of the vector area element $\mathrm{d}\boldsymbol{A}$ defined at point $\boldsymbol{x}\,(x_1,\ x_2,\ x_3)$ on the dislocation surface A. The above $w_{\mathrm{FS}}^{[\lambda]}$ is the self-energy of the dislocation loop C in a transversely isotropic MEE full space occupied by material λ, and $W_{\mathrm{IS}}^{[\lambda]}$ is the image self-energy from the image sources due to the bimaterial interface.

Following the derivation of (36), similarly, we can obtain from (43) that

$$\begin{aligned} w_{\mathrm{FS}}^{[\lambda]} &= \frac{1}{8\pi} \sum_{I,J=1}^{5} b_I b_J \oint_C \mathrm{d}x_I \oint_C \mathrm{d}y_J C_I^{[\lambda]} \mathcal{W}_J^{[\lambda]}(\boldsymbol{y};\boldsymbol{x}) \\ &\quad - \frac{1}{8\pi} \sum_{I,J=1}^{5} \sum_{m,n,p,q=1}^{3} b_I b_J \oint_C \mathrm{d}x_m \oint_C \mathrm{d}y_n \varepsilon_{pIm} \varepsilon_{qJn} \frac{\partial^2}{\partial x_p \partial y_q} C_I^{[\lambda]} \mathcal{S}^{[\lambda]}_{pI;qJ}(\boldsymbol{y};\boldsymbol{x}), \end{aligned} \tag{44a}$$

and

$$W_{\rm IS}^{[\lambda]} = -\frac{1}{4\pi}\sum_{I,J=1}^{5}\sum_{k,p,q=1}^{3} b_I b_J \oint_C \mathrm{d}x_p \oint_C \mathrm{d}y_q \varepsilon_{IJk}\varepsilon_{pqk} C_I^{[\lambda]}\mathcal{W}_{Jq}^{[\lambda][\lambda]}(\boldsymbol{y};\boldsymbol{x})$$
$$+\frac{1}{8\pi}\sum_{I,J=1}^{5} b_I b_J \oint_C \mathrm{d}x_I \oint_C \mathrm{d}y_J C_I^{[\lambda]}\mathcal{W}_{J}^{[\lambda][\lambda]}(\boldsymbol{y};\boldsymbol{x}) - \frac{1}{8\pi}\sum_{I,J=1}^{5}\sum_{m,n,p,q=1}^{3} b_I b_J$$
$$\cdot \oint_C \mathrm{d}x_m \oint_C \mathrm{d}y_n \varepsilon_{pIm}\varepsilon_{qJn}\frac{\partial^2}{\partial x_p \partial y_q} C_I^{[\lambda]}\mathcal{S}_{pI;qJ}^{[\lambda][\lambda]}(\boldsymbol{y};\boldsymbol{x}). \tag{44b}$$

In summary, we have presented line-integral expressions for the extended displacements, extended stresses, interaction energy, and self-energy of arbitrarily shaped 3D dislocation loops in transversely isotropic MEE bimaterials, as shown in (22), (27), (36), (44a), and (44b). These line-integral expressions are the main results of this paper.

4 Numerical examples and discussion

In this section, we utilize our dislocation solutions in Section 3 to investigate the multi-field coupling effect and the interface/surface effect in transversely isotropic MEE materials. Before presenting the numerical examples, we point out that our formulations have been verified to be correct by comparing our numerical results with those in Han and Pan[18].

Example 1 The extended displacements and extended stresses of a cardioid dislocation loop in transversely isotropic MEE bimaterials.

In the Cartesian coordinates, we consider a transversely isotropic bimaterial which is composed of the MEE $BaTiO_3$-$CoFe_2O_4$ (material 1, $x_3 > 0$) and the piezoelectric $BaTiO_3$ (material 2, $x_3 < 0$), with the isotropic plane of both materials being parallel to the perfectly bonded interface (i.e., x_3=0). The MEE $BaTiO_3$-$CoFe_2O_4$ composite is based on the 25% $BaTiO_3$ and 75% $CoFe_2O_4$. The material coefficients used here are listed as follows[9]:

$c_{11} = 245,\quad c_{33} = 235,\quad c_{44} = 47.6,\quad c_{13} = 138,\quad c_{66} = 53\ \mathrm{GPa},\quad e_{31} = -1.53,\quad e_{33} = 4.28,$

$e_{15} = 0.05\ \mathrm{C\cdot m^{-2}},\quad q_{31} = 378,\quad q_{33} = 476,\quad q_{15} = 331.2\ \mathrm{N\cdot A^{-1}\cdot m^{-1}},\quad \varepsilon_{11} = 0.13,$

$\varepsilon_{33} = 3.24\times 10^{-9}\,\mathrm{F\cdot m^{-1}},\quad \mu_{11} = 3.57,\quad \mu_{33} = 1.21\times 10^{-4}\,\mathrm{H\cdot m^{-1}},\quad d_{11} = -3.09,$

$d_{33} = 2\,334.15\times 10^{-12}\,\mathrm{s\cdot m^{-1}}$ for the MEE $BaTiO_3$-$CoFe_2O_4$,

$c_{11} = 166,\quad c_{33} = 162,\quad c_{44} = 43,\quad c_{13} = 78,$

$c_{66} = 44.5\ \mathrm{GPa},\quad e_{31} = -4.4,\quad e_{33} = 18.6,\quad e_{15} = 11.6\ \mathrm{C\cdot m^{-2}},$

$q_{31} = q_{33} = q_{15} = 0,\quad \varepsilon_{11} = 11.2,\quad \varepsilon_{33} = 12.6\times 10^{-9}\,\mathrm{F\cdot m^{-1}},\quad \mu_{11} = 0.05,$

$\mu_{33} = 0.1\times 10^{-4}\,\mathrm{H\cdot m^{-1}},\quad d_{11} = d_{33} = 0$ for the piezoelectric $BaTiO_3$.

We consider a cardioid dislocation loop C_1 whose parametric equation is described by

$$\begin{cases} x_1(t) = a(1+\cos t)\cos t, \\ x_2(t) = a(1+\cos t)\sin t, \quad 0 \leqslant t \leqslant 2\pi, \quad a > 0, \\ x_3 = h \end{cases} \tag{45}$$

with h being a real constant and a being the shape parameter of the cardioid (see Fig. 2). In this example, the cardioid dislocation loop is assumed to be located on the plane $x_3 = h = 0.5a$ in material 1 (i.e., MEE $BaTiO_3$-$CoFe_2O_4$).

Shown in Figs. 3 and 4 are the electric potential ϕ, magnetic potential ψ, electric displacement component D_3, and magnetic induction component B_3 on a vertical line (i.e., $x_1 = 0$,

$x_2 = 0.5a$, $-4a \leqslant x_3 \leqslant 5a$) due to the loop C_1 with an extended Burgers vector (0, 0, 0, $\Delta\phi_1$, 0) or (0, 0, 0, 0, $\Delta\psi_1$). Three different cases are investigated, in which the loop C_1 is located in the perfectly-bonded MEE bimaterial as mentioned above, an MEE $BaTiO_3$-$CoFe_2O_4$ half space ($x_3 \geqslant 0$) with a free surface at $x_3 = 0$ (see Appendix B), and MEE $BaTiO_3$-$CoFe_2O_4$ full space. It can be observed from Figs. 3 and 4 that the curves are very sensitive to different boundary conditions except for those in Figs. 3(d) and 4(d). This is mainly caused by the fact that $BaTiO_3$ (i.e., material 2) has relatively large dielectric and piezoelectric coefficients while but extremely small piezomagnetic and magnetic-permeability coefficients. In addition, Figs. 3(b), 3(c), 4(b), and (4c) show an obvious ME coupling effect in MEE materials.

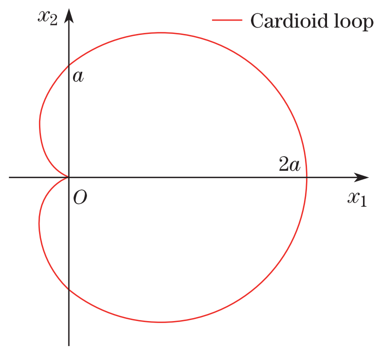

Fig. 2 Schematic of cardioid dislocation loop C_1 described by (45)

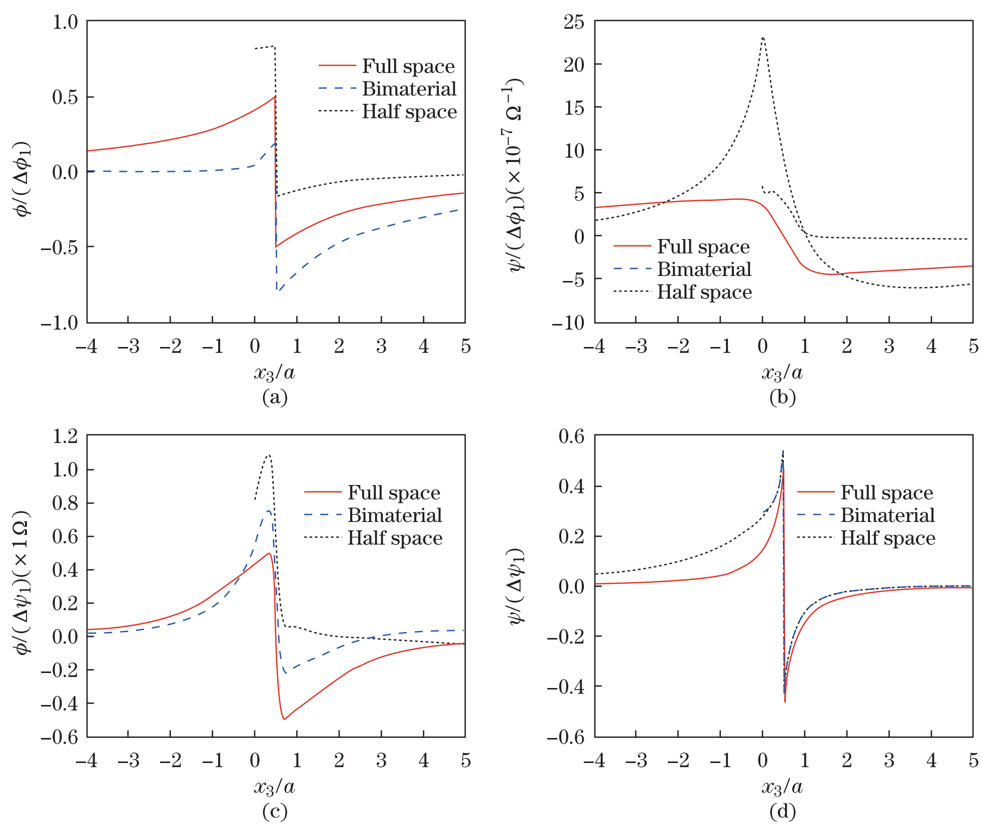

Fig. 3 Electric potential ϕ or magnetic potential ψ on vertical line (i.e., $x_1 = 0$, $x_2 = 0.5a$, $-4a \leqslant x_3 \leqslant 5a$) due to the cardioid loop C_1 with extended Burgers vector (0, 0, 0, $\Delta\phi_1$, 0) or (0, 0, 0, 0, $\Delta\psi_1$): (a) $\phi \sim$ (0, 0, 0, $\Delta\phi_1$, 0); (b) $\psi \sim$ (0, 0, 0, $\Delta\phi_1$, 0); (c) $\phi \sim$ (0, 0, 0, 0, $\Delta\psi_1$); (d) $\psi \sim$ (0, 0, 0, 0, $\Delta\psi_1$)

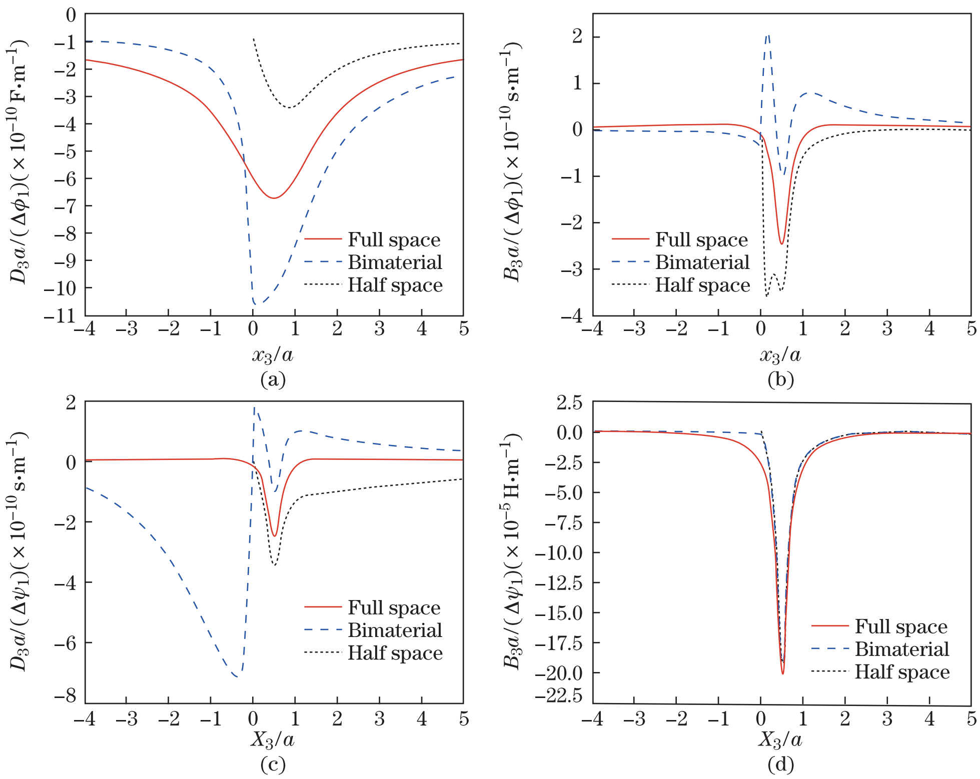

Fig. 4 Electric displacement component D_3 or magnetic induction component B_3 on vertical line (i.e., $x_1 = 0$, $x_2 = 0.5a$, $-4a \leqslant x_3 \leqslant 5a$) due to cardioid loop C_1 with extended Burgers vector (0, 0, 0, $\Delta\phi_1$, 0) or (0, 0, 0, 0, $\Delta\psi_1$): (a) $D_3 \sim$ (0, 0, 0, $\Delta\phi_1$, 0); (b) $B_3 \sim$ (0, 0, 0, $\Delta\phi_1$, 0); (c) $D_3 \sim$ (0, 0, 0, 0, $\Delta\psi_1$); (d) $B_3 \sim$ (0, 0, 0, 0, $\Delta\psi_1$)

Example 2 The interaction energy between two cardioid dislocation loops in transversely isotropic MEE bimaterials

In this example, we investigate the influence of the bimaterial interface and the half-space surface on the interaction energy between two cardioid dislocation loops C_1 and C_2 in MEE materials. The models of the MEE bimaterial, half space ($x_3 \geqslant 0$) and full space are exactly the same as those in Example 1. The first loop C_1 with the extended Burgers vector (0, 0, 0, $\Delta\phi_1$, 0) or (0, 0, 0, 0, $\Delta\psi_1$) is also described by (45) with $h = 0.5a$. The second loop C_2 with the extended Burgers vector (0, 0, 0, $\Delta\phi_2$, 0) or (0, 0, 0, 0, $\Delta\psi_2$) is described by the following parametric equation:

$$\begin{cases} x_1(t) = a(1+\cos t)\cos t + a, \\ x_2(t) = a(1+\cos t)\sin t + a, \quad 0 \leqslant t \leqslant 2\pi, \quad a > 0, \\ x_3 = X_3 \end{cases} \tag{46}$$

with X_3 being independent of the parameter t. It is noted that (46) is just a simple translation relative to (45).

The numerical results for the interaction energy between loops C_1 and C_2 are shown in Fig. 5. Similarly to Figs. 3 and 4 in Example 1, the interaction energy in Fig. 5 is also sensitive to different boundary conditions, and an obvious ME coupling effect is also observed.

Example 3 The image self-energy of a cardioid dislocation loop in transversely isotropic MEE bimaterials

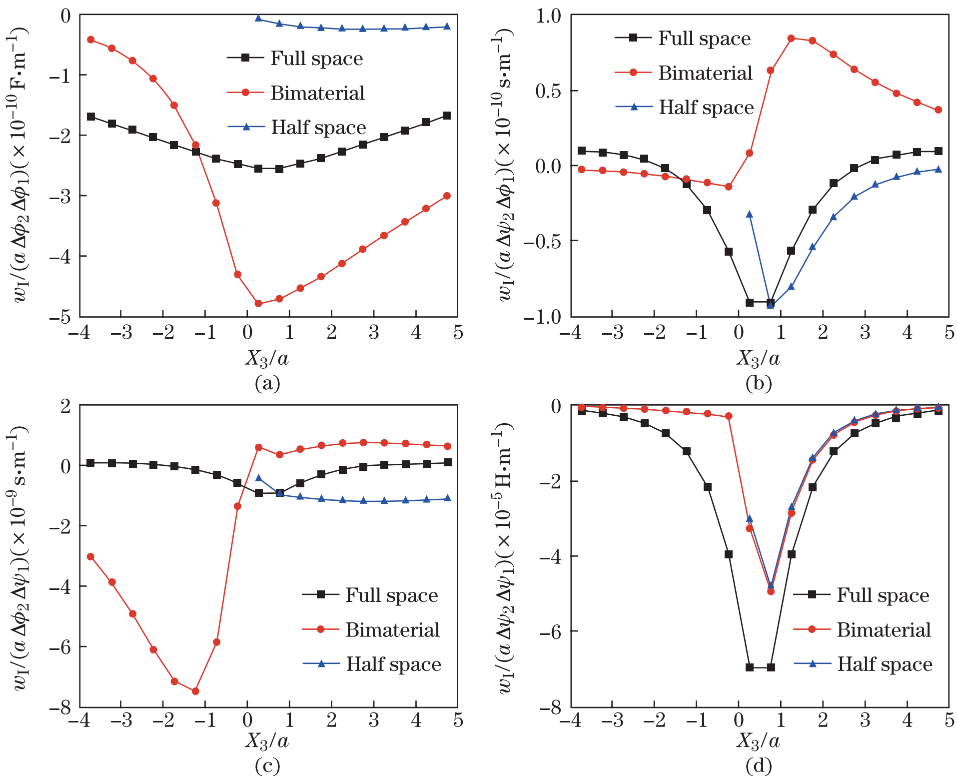

Fig. 5 Influence of location of loop C_2 (i.e., X_3) on interaction energy w_I between loop C_1 described by (45) with extended Burgers vector (0, 0, 0, $\Delta\phi_1$, 0) or (0, 0, 0, 0, $\Delta\psi_1$) and loop C_2 described by (46) with extended Burgers vector (0, 0, 0, $\Delta\phi_2$, 0) or (0, 0, 0, 0, $\Delta\psi_2$): (a) $w_I \sim$ (0, 0, 0, $\Delta\phi_1$, 0) and (0, 0, 0, $\Delta\phi_2$, 0); (b) $w_I \sim$ (0, 0, 0, $\Delta\phi_1$, 0) and (0, 0, 0, 0, $\Delta\psi_2$); (c) $w_I \sim$ (0, 0, 0, 0, $\Delta\psi_1$) and (0, 0, 0, $\Delta\phi_2$, 0); (d) $w_I \sim$ (0, 0, 0, 0, $\Delta\psi_1$) and (0, 0, 0, 0, $\Delta\psi_2$)

In this example, the model of the MEE bimaterial is also exactly the same as in Example 1. An MEE $BaTiO_3$-$CoFe_2O_4$ half space ($x_3 \geqslant 0$) and a piezoelectric $BaTiO_3$ half space ($x_3 \leqslant 0$), both with a free surface at $x_3 = 0$, are also considered here.

We first investigate the influence of the distance between the interface/surface and the cardioid dislocation loop C_2 on its image self-energy. Here, the cardioid loop C_2 is also described by (46), with its extended Burgers vector being (0, 0, 0, $\Delta\phi_2$, 0) or (0, 0, 0, 0, $\Delta\psi_2$). The numerical results are shown in Fig. 6. It can be observed from Fig. 6 that (i) for the loop C_2 with an extended Burgers vector (0, 0, 0, $\Delta\phi_2$, 0), the perfect bimaterial interface imposes an attractive force upon this loop if it is located within MEE $BaTiO_3$-$CoFe_2O_4$ which exhibits a relatively weaker piezoelectric effect, and imposes a repulsive force upon this loop if it is located within $BaTiO_3$ which exhibits a relatively stronger piezoelectric effect; (ii) for the loop C_2 with an extended Burgers vector (0, 0, 0, 0, $\Delta\psi_2$), the perfect bimaterial interface imposes a repulsive force upon this loop if it is located within MEE $BaTiO_3$-$CoFe_2O_4$ which exhibits a relatively stronger piezomagnetic effect, and imposes an attractive force upon this loop if it is located within $BaTiO_3$ which exhibits a relatively weaker piezomagnetic effect; (iii) for the loop C_2 with an extended Burgers vector either (0, 0, 0, $\Delta\phi_2$, 0) or (0, 0, 0, 0,$\Delta\psi_2$), the free surface always imposes a repulsive force upon this loop. In other words, if the interface or surface is present, the dislocation loop with an electric-potential (or a magnetic-potential) discontinuity always has the tendency to move towards the material with a relatively stronger piezoelectric (or piezomagnetic) effect. This phenomenon in MEE materials is quite different from that for dislocation loops in purely elastic materials[3].

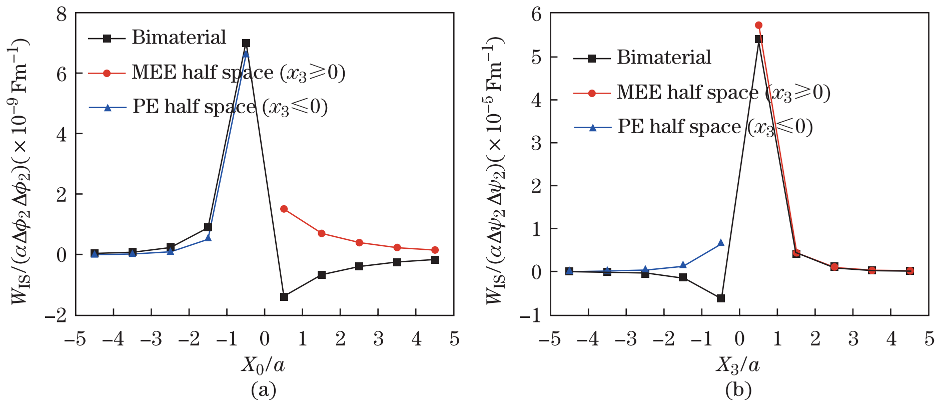

Fig. 6 Influence of location of loop C_2 (i.e., X_3) on image self-energy W_{IS} of loop C_2 described by (46) with extended Burgers vector (0, 0, 0, $\Delta\phi_2$, 0) or (0, 0, 0, 0, $\Delta\psi_2$): (a) $W_{\mathrm{IS}} \sim$ (0, 0, 0, $\Delta\phi_2$, 0); (b) $W_{\mathrm{IS}} \sim$ (0, 0, 0, 0, $\Delta\psi_2$) ("PE" is abbreviation for "piezoelectric")

Then, we investigate the influence of the size of the cardioid dislocation loop C_1 on its image self-energy. Here, the cardioid loop C_1 with an extended Burgers vector (0, 0, 0, $\Delta\phi_1$, 0) or (0, 0, 0, 0, $\Delta\psi_1$) is also described by (45) with $h = 0.5a_0$ or $-0.5a_0$ (a_0 = const. > 0), but we change the size of this cardioid loop by simply changing its shape parameter a. The numerical results are shown in Fig. 7. It can be observed from Fig. 7 that (i) for the loop C_1 with an extended Burgers vector (0, 0, 0, $\Delta\phi_1$, 0), the perfect bimaterial interface imposes an expanding force upon this loop if it is located within MEE $BaTiO_3$-$CoFe_2O_4$ which exhibits a relatively weaker piezoelectric effect, and imposes a shrinking force upon this loop if it is located within $BaTiO_3$ which exhibits a relatively stronger piezoelectric effect; (ii) for the loop C_1 with an extended Burgers vector (0, 0, 0, 0, $\Delta\psi_1$), the perfect bimaterial interface imposes a shrinking force upon this loop if it is located within MEE $BaTiO_3$-$CoFe_2O_4$ which exhibits a relatively stronger piezomagnetic effect, and imposes an expanding force upon this loop if it is located within $BaTiO_3$ which exhibits a relatively weaker piezomagnetic effect; (iii) for the loop C_1 with an extended Burgers vector either (0, 0, 0, $\Delta\phi_1$, 0) or (0, 0, 0, 0, $\Delta\psi_1$), the free surface always imposes a shrinking force upon this loop.

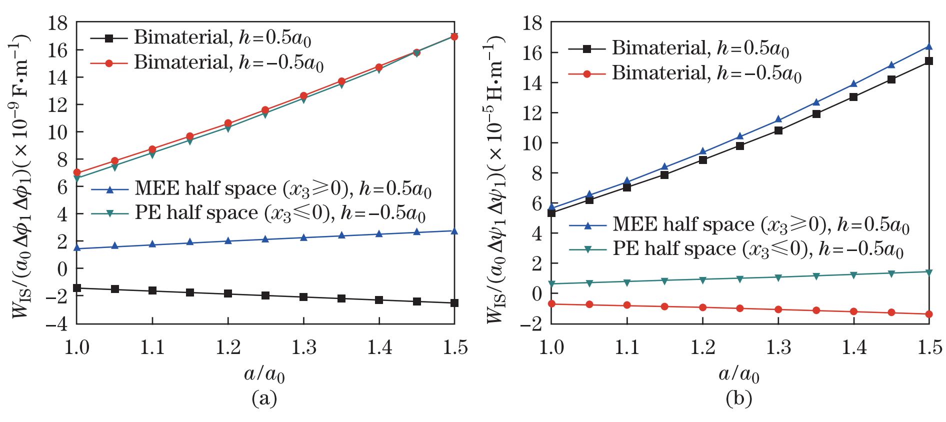

Fig. 7 Influence of size of loop C_1 on image self-energy of loop C_1 described by (45) with extended Burgers vector (0, 0, 0, $\Delta\phi_1$, 0) or (0, 0, 0, 0, $\Delta\psi_1$): (a) $W_{\mathrm{IS}} \sim$ (0, 0, 0, $\Delta\phi_1$, 0); (b) $W_{\mathrm{IS}} \sim$ (0, 0, 0, 0, $\Delta\psi_1$) ("PE" is abbreviation for "piezoelectric")

5 Conclusions

In this paper, we derive simple and elegant line-integral expressions for the extended displacements, extended stresses, interaction energy, and self-energy of arbitrarily shaped 3D dislocation loops with constant extended Burgers vector in transversely isotropic MEE bimaterials. These expressions are very similar to their elastic isotropic full-space counterparts, such as Burgers' formula for displacements[19], Peach-Koehler's formula for stresses[20], and Blin's formula for the interaction energy[21]. Moreover, it is straightforward to reduce our line-integral expressions for MEE materials to those for piezoelectric, piezomagnetic, or purely elastic materials.

Our line-integral expressions for transversely isotropic MEE bimaterials are also suitable for a transversely isotropic MEE half space, provided that we slightly modify some coefficients of the point-force Green's function for bimaterials, as shown in Appendix B.

All possible degenerate cases of these expressions can be treated systematically via proper limiting processes[3]. In numerical calculations, we can also deal with these degenerate cases by means of a slight perturbation to material coefficients.

Our numerical examples show clearly the multi-field coupling and interface/surface effects on the extended displacements, extended stresses, and interaction energy of dislocation loops in the MEE materials. It is also observed from Example 3 that, for a dislocation loop with an electric-potential (or a magnetic-potential) discontinuity, the bimaterial interface would impose repulsive and shrinking forces to the dislocation loop embedded in the MEE material with a relatively stronger piezoelectric (or piezomagnetic) effect, while it would impose attractive and expanding forces to the dislocation loop embedded in the MEE material with a relatively weaker piezoelectric (or piezomagnetic) effect; however, the half-space surface would always impose repulsive and shrinking forces to the dislocation loop.

Acknowledgements The first author would like to dedicate this paper to the late Professor Y. H. PAO from College of Civil Engineering and Architecture in Zhejiang University for his supervision.

References

[1] Nan, C. W., Bichurin, M. I., Dong, S. X., Viehland, D., and Srinivasan, G. Multiferroic magnetoelectric composites: historical perspective, status, and future directions. *Journal of Applied Physics*, **103**, 031101 (2008)

[2] Ma, J., Hu, J. M., Li, Z., and Nan, C. W. Recent progress in multiferroic magnetoelectric composites: from bulk to thin films. *Advanced Materials*, **23**, 1062–1087 (2011)

[3] Yuan, J. H., Pan, E., and Chen, W. Q. Line-integral representations for the elastic displacements, stresses and interaction energy of arbitrary dislocation loops in transversely isotropic bimaterials. *International Journal of Solids and Structures*, **50**, 3472–3489 (2013)

[4] Chu, H. J., Pan, E., Han, X., Wang, J., and Beyerlein, I. J. Elastic fields of dislocation loops in three-dimensional anisotropic bimaterials. *Journal of the Mechanics and Physics of Solids*, **60**, 418–431 (2012)

[5] Chu, H. J., Pan, E., Wang, J., and Beyerlein, I. J. Elastic displacement and stress fields induced by a dislocation of polygonal shape in an anisotropic elastic half-space. *Journal of Applied Mechanics*, **79**, 1–9 (2012)

[6] Akarapu, S. and Zbib, H. M. Line-integral solution for the stress and displacement fields of an arbitrary dislocation segment in isotropic bi-materials in 3D space. *Philosophical Magazine*, **89**, 2149–2166 (2009)

[7] Tan, E. H. and Sun, L. Z. Stress field due to a dislocation loop in a heterogeneous thin film-substrate system. *Modelling and Simulation in Materials Science and Engineering*, **14**, 993–1013 (2006)

[8] Gosling, T. J. and Willis, J. R. A line-integral representation for the stresses due to an arbitrary dislocation in an isotropic half-space. *Journal of the Mechanics and Physics of Solids*, **42**, 1199–1221 (1994)

[9] Han, X. L., Pan, E., and Sangghaleh, A. Fields induced by three-dimensional dislocation loops in anisotropic magneto-electro-elastic bimaterials. *Philosophical Magazine*, **93**, 3291–3313 (2013)

[10] Chen, W. Q., Pan, E., Wang, H. M., and Zhang, C. Z. Theory of indentation on multiferroic composite materials. *Journal of the Mechanics and Physics of Solids*, **58**, 1524–1551 (2010)

[11] Hou, P. F., Ding, H. J., and Chen, J. Y. Green's functions for transversely isotropic magnetoelectroelastic media. *International Journal of Engineering Science*, **43**, 826–858 (2005)

[12] Chen, W. Q., Lee, K. Y., and Ding, H. J. General solution for transversely isotropic magneto-electro-thermo-elasticity and the potential theory method. *International Journal of Engineering Science*, **42**, 1361–1379 (2004)

[13] Ding, H. J., Chen, W. Q., and Zhang, L. C. *Elasticity of Transversely Isotropic Materials*, Springer, New York (2006)

[14] Fabrikant, V. I. A new form of the Green function for a transversely isotropic body. *Acta Mechanica*, **167**, 101–111 (2004)

[15] Hirth, J. P. and Lothe, J. *Theory of Dislocations*, John Wiley & Sons, New York (1982)

[16] Mura, T. *Micromechanics of Defects in Solids*, Martinus-Nijhoff Publishers, Dordrecht (1987)

[17] Yuan, J. H., Chen, W. Q., and Pan, E. Line-integral representations of the displacement and stress fields due to an arbitrary Volterra dislocation loop in a transversely isotropic elastic full space. *International Journal of Solids and Structures*, **50**, 160–175 (2013)

[18] Han, X. L. and Pan, E. Fields produced by three-dimensional dislocation loops in anisotropic magneto-electro-elastic materials. *Mechanics of Materials*, **59**, 110–125 (2013)

[19] Burgers, J. M. Some considerations on the fields of stress connected with dislocations in a regular crystal lattice. *Koninklijke Nederlandse Akademie van Wetenschappen*, **42**, 293–325 (1939)

[20] Peach, M. and Koehler J. S. The forces exerted on dislocations and the stress fields produced by them. *Physical Review*, **80**, 436–439 (1950)

[21] Blin, J. Energie mutuelle de deux dislocations. *Acta Metallurgica*, **3**, 199–200 (1955)

[22] Barnett, D. M. and Lothe, J. Dislocations and line charges in anisotropic piezoelectric insulators. *Physica Status Solidi*, **67b**, 105–111 (1975)

[23] Pan, E. Three-dimensional Green's functions in anisotropic magneto-electro-elastic bimaterials. *Zeitschrift für Angewandte Mathematik und Physik*, **53**, 815–838 (2002)

Appendix A General solutions of coupled equations for transversely isotropic MEE media

Using the extended Barnett and Lothe notation[22–23], in Cartesian coordinates (x_1, x_2, x_3), the governing equations and constitutive relations for transversely isotropic MEE media can be expressed as

$$f_J(\boldsymbol{x})+\sum_{K=1}^{5}\sum_{i,l=1}^{3}c_{iJKl}\frac{\partial^2}{\partial x_l\partial x_i}u_K(\boldsymbol{x})=0, \tag{A1a}$$

$$\sigma_{iJ}(\boldsymbol{x})=\sum_{K=1}^{5}\sum_{l=1}^{3}c_{iJKl}\frac{\partial}{\partial x_l}u_K(\boldsymbol{x}), \tag{A1b}$$

in which the extended body force, extended displacement, and extended stress are defined as

$$f_I=\begin{cases} f_i, & I=i=1,2,3,\\ -f_{\mathrm{e}}, & I=4,\\ -f_{\mathrm{m}}, & I=5,\end{cases}\qquad u_I=\begin{cases} u_i, & I=i=1,2,3,\\ \phi, & I=4,\\ \psi, & I=5,\end{cases}\qquad \sigma_{iJ}=\begin{cases} \sigma_{ij}, & J=j=1,2,3,\\ D_i, & J=4,\\ B_i, & J=5,\end{cases} \tag{A2}$$

where f_i, f_{e}, and f_{m} are the body force, electric charge, and electric current (or called magnetic charge), respectively; u_i, ϕ, and ψ are the elastic displacement, electric potential, and magnetic potential, respectively; σ_{ij}, D_i, and B_i are the stress, electric displacement, and magnetic induction, respectively.

Also in (A1a) and (A1b), the extended elastic coefficient tensor for transversely isotropic MEE media can be written as

$$c_{iJKl} = \begin{cases} c_{ijkl}, \quad J=j=1,2,3, \quad K=k=1,2,3, \\ e_{lij}, \quad J=j=1,2,3, \quad K=4, \\ e_{ikl}, \quad J=4, \quad K=k=1,2,3, \\ q_{lij}, \quad J=j=1,2,3, \quad K=5, \\ q_{ikl}, \quad J=5, \quad K=k=1,2,3, \\ -d_{il}, \quad J=4, \quad K=5 \quad \text{or} \quad J=5, \quad K=4, \\ -\varepsilon_{il}, \quad J=4, \quad K=4, \\ -\mu_{il}, \quad J=5, \quad K=5, \end{cases} \tag{A3a}$$

where c_{ijkl}, ε_{ij}, and μ_{ij} are the elastic, dielectric, and magnetic permeability coefficients, respectively; e_{ijk}, q_{ijk}, and d_{ij} are the piezoelectric, piezomagnetic, and magnetoelectric coefficients, respectively. If the isotropic plane of the transversely isotropic MEE medium is parallel to the x_1x_2-plane, then the above coefficients can be expressed explicitly as

$$\begin{cases} c_{ijkl} = (c_{11}-2c_{66})\delta_{ij}\delta_{kl} + c_{66}(\delta_{ik}\delta_{jl}+\delta_{il}\delta_{jk}) \\ \qquad\quad + (c_{11}+c_{33}-2c_{13}-4c_{44})\delta_{i3}\delta_{j3}\delta_{k3}\delta_{l3} \\ \qquad\quad + (c_{13}-c_{11}+2c_{66})(\delta_{i3}\delta_{j3}\delta_{kl}+\delta_{k3}\delta_{l3}\delta_{ij}) \\ \qquad\quad + (c_{44}-c_{66})(\delta_{j3}\delta_{k3}\delta_{il}+\delta_{i3}\delta_{l3}\delta_{jk}+\delta_{j3}\delta_{l3}\delta_{ik}+\delta_{i3}\delta_{k3}\delta_{jl}), \\ e_{lij} = e_{31}\delta_{ij}\delta_{l3} + e_{15}(\delta_{il}\delta_{j3}+\delta_{i3}\delta_{jl}) + (e_{33}-e_{31}-2e_{15})\delta_{i3}\delta_{j3}\delta_{l3}, \\ q_{lij} = q_{31}\delta_{ij}\delta_{l3} + q_{15}(\delta_{il}\delta_{j3}+\delta_{i3}\delta_{jl}) + (q_{33}-q_{31}-2q_{15})\delta_{i3}\delta_{j3}\delta_{l3}, \\ \varepsilon_{ij} = \varepsilon_{11}\delta_{ij} + (\varepsilon_{33}-\varepsilon_{11})\delta_{i3}\delta_{j3}, \\ \mu_{ij} = \mu_{11}\delta_{ij} + (\mu_{33}-\mu_{11})\delta_{i3}\delta_{j3}, \\ d_{ij} = d_{11}\delta_{ij} + (d_{33}-d_{11})\delta_{i3}\delta_{j3}, \end{cases} \tag{A3b}$$

where c_{mn}, e_{in}, and q_{in} (m, n=1, 2, 3, 4, 5, 6) are the contracted elastic, piezoelectric, and piezomagnetic coefficients; δ_{ij} is the 3×3 Kronecker delta.

According to Hou et al.[11] and Chen et al.[12], the general solution of (A1a) and (A1b) can be expressed compactly as

$$\begin{cases} u_1(\boldsymbol{x}) + \mathrm{i}u_2(\boldsymbol{x}) = \Big(\dfrac{\partial}{\partial x_1} + \mathrm{i}\dfrac{\partial}{\partial x_2}\Big)\Big(\mathrm{i}\Psi_5(\boldsymbol{x}) + \displaystyle\sum_{n=1}^{4}\Psi_n(\boldsymbol{x})\Big), \\ u_{j+2}(\boldsymbol{x}) = \dfrac{\partial}{\partial x_3}\displaystyle\sum_{n=1}^{4} m_{nj}\Psi_n(\boldsymbol{x}) = \dfrac{\partial}{\partial x_3}\displaystyle\sum_{n=1}^{4}\alpha_{nj}\gamma_n\Psi_n(\boldsymbol{x}), \end{cases} \tag{A4a}$$

and

$$\begin{cases} \sigma_{11}(\boldsymbol{x}) + \sigma_{22}(\boldsymbol{x}) = \Big(\dfrac{\partial^2}{\partial x_1^2} + \dfrac{\partial^2}{\partial x_2^2}\Big)\displaystyle\sum_{n=1}^{4} 2\Big(\omega_{n1}s_n - c_{66}\Big)\Psi_n(\boldsymbol{x}), \\ \sigma_{11}(\boldsymbol{x}) - \sigma_{22}(\boldsymbol{x}) + 2\mathrm{i}\sigma_{12}(\boldsymbol{x}) = 2c_{66}\Big(\dfrac{\partial}{\partial x_1} + \mathrm{i}\dfrac{\partial}{\partial x_2}\Big)^2\Big(\mathrm{i}\Psi_5(\boldsymbol{x}) + \displaystyle\sum_{n=1}^{4}\Psi_n(\boldsymbol{x})\Big), \\ \sigma_{1(j+2)}(\boldsymbol{x}) + \mathrm{i}\sigma_{2(j+2)}(\boldsymbol{x}) = \dfrac{\partial}{\partial x_3}\Big(\dfrac{\partial}{\partial x_1} + \mathrm{i}\dfrac{\partial}{\partial x_2}\Big)\Big(\mathrm{i}C_{j+2}\Psi_5(\boldsymbol{x}) + \displaystyle\sum_{n=1}^{4}\omega_{nj}\gamma_n\Psi_n(\boldsymbol{x})\Big), \\ \sigma_{3(j+2)}(\boldsymbol{x}) = -\Big(\dfrac{\partial^2}{\partial x_1^2} + \dfrac{\partial^2}{\partial x_2^2}\Big)\displaystyle\sum_{n=1}^{4}\theta_{nj}\Psi_n(\boldsymbol{x}), \quad \sigma_{ij}(\boldsymbol{x}) = \sigma_{ji}(\boldsymbol{x}), \end{cases} \tag{A4b}$$

where $\mathrm{i} = \sqrt{-1}$, Ψ_J satisfies the quasi-harmonic equations as follows:

$$\Big(\frac{\partial^2}{\partial x_1^2} + \frac{\partial^2}{\partial x_2^2} + \gamma_J^2\frac{\partial^2}{\partial x_3^2}\Big)\Psi_J(\boldsymbol{x}) = 0 \tag{A5}$$

with

$$\gamma_5 \equiv 1/s_5 = \sqrt{c_{44}/c_{66}}, \quad \gamma_n \equiv 1/s_n \ (n = 1, 2, 3, 4). \tag{A6}$$

In (A4b), (A5), and (A6), γ_n (n=1,2,3,4) satisfies the following characteristic equation:

$$\det\left(\mathbf{\Pi}_n\right) = 0 \ (n = 1, 2, 3, 4), \tag{A7}$$

where

$$\mathbf{\Pi}_n = \mathbf{\Pi}(\gamma_n) = \begin{pmatrix} c_{44} - c_{11}\gamma_n^2 & -(c_{44} + c_{13}) & -(e_{15} + e_{31}) & -(q_{15} + q_{31}) \\ (c_{44} + c_{13})\gamma_n^2 & c_{33} - c_{44}\gamma_n^2 & e_{33} - e_{15}\gamma_n^2 & q_{33} - q_{15}\gamma_n^2 \\ -(e_{15} + e_{31})\gamma_n^2 & e_{15}\gamma_n^2 - e_{33} & \varepsilon_{33} - \varepsilon_{11}\gamma_n^2 & d_{33} - d_{11}\gamma_n^2 \\ -(q_{15} + q_{31})\gamma_n^2 & q_{15}\gamma_n^2 - q_{33} & d_{33} - d_{11}\gamma_n^2 & \mu_{33} - \mu_{11}\gamma_n^2 \end{pmatrix} (n = 1, 2, 3, 4). \tag{A8}$$

In other words, γ_n (n=1,2,3,4) are the four roots (with positive real part) of the following algebraic equation:

$$\det(\mathbf{\Pi}(\gamma)) = n_4(\gamma^2)^4 - n_3(\gamma^2)^3 + n_2(\gamma^2)^2 - n_1(\gamma^2) + n_0 = 0, \tag{A9}$$

where

$$n_0 = -c_{44}\det\begin{pmatrix} -c_{33} & e_{33} & q_{33} \\ e_{33} & \varepsilon_{33} & d_{33} \\ q_{33} & d_{33} & \mu_{33} \end{pmatrix}, \quad n_4 = -c_{11}\det\begin{pmatrix} -c_{44} & e_{15} & q_{15} \\ e_{15} & \varepsilon_{11} & d_{11} \\ q_{15} & d_{11} & \mu_{11} \end{pmatrix}, \tag{A10a}$$

$$\begin{aligned} n_1 = {} & \det\begin{pmatrix} -c_{11} & -(c_{13} + c_{44}) & (e_{15} + e_{31}) & (q_{15} + q_{31}) \\ -(c_{13} + c_{44}) & -c_{33} & e_{33} & q_{33} \\ (e_{15} + e_{31}) & e_{33} & \varepsilon_{33} & d_{33} \\ (q_{15} + q_{31}) & q_{33} & d_{33} & \mu_{33} \end{pmatrix} - c_{44}\det\begin{pmatrix} -c_{44} & e_{33} & q_{33} \\ e_{15} & \varepsilon_{33} & d_{33} \\ q_{15} & d_{33} & \mu_{33} \end{pmatrix} \\ & - c_{44}\det\begin{pmatrix} -c_{33} & e_{15} & q_{33} \\ e_{33} & \varepsilon_{11} & d_{33} \\ q_{33} & d_{11} & \mu_{33} \end{pmatrix} - c_{44}\det\begin{pmatrix} -c_{33} & e_{33} & q_{15} \\ e_{33} & \varepsilon_{33} & d_{11} \\ q_{33} & d_{33} & \mu_{11} \end{pmatrix}, \end{aligned}$$

$$\begin{aligned} n_3 = {} & \det\begin{pmatrix} -c_{44} & -(c_{13} + c_{44}) & (e_{15} + e_{31}) & (q_{15} + q_{31}) \\ -(c_{13} + c_{44}) & -c_{44} & e_{15} & q_{15} \\ (e_{15} + e_{31}) & e_{15} & \varepsilon_{11} & d_{11} \\ (q_{15} + q_{31}) & q_{15} & d_{11} & \mu_{11} \end{pmatrix} - c_{11}\det\begin{pmatrix} -c_{33} & e_{33} & q_{33} \\ e_{15} & \varepsilon_{11} & d_{11} \\ q_{15} & d_{11} & \mu_{11} \end{pmatrix} \\ & - c_{11}\det\begin{pmatrix} -c_{44} & e_{15} & q_{15} \\ e_{33} & \varepsilon_{33} & d_{33} \\ q_{15} & d_{11} & \mu_{11} \end{pmatrix} - c_{11}\det\begin{pmatrix} -c_{44} & e_{15} & q_{15} \\ e_{15} & \varepsilon_{11} & d_{11} \\ q_{33} & d_{33} & \mu_{33} \end{pmatrix}, \end{aligned} \tag{A10b}$$

$$\begin{aligned} n_2 = {} & \det\begin{pmatrix} -c_{11} & 0 & (e_{15} + e_{31}) & (q_{15} + q_{31}) \\ -(c_{13} + c_{44}) & -c_{44} & e_{33} & q_{33} \\ (e_{15} + e_{31}) & e_{15} & \varepsilon_{33} & d_{33} \\ (q_{15} + q_{31}) & q_{15} & d_{33} & \mu_{33} \end{pmatrix} - c_{44}\det\begin{pmatrix} -c_{44} & e_{33} & q_{15} \\ e_{15} & \varepsilon_{33} & d_{11} \\ q_{15} & d_{33} & \mu_{11} \end{pmatrix} \\ & + \det\begin{pmatrix} -c_{11} & -(c_{13} + c_{44}) & 0 & (q_{15} + q_{31}) \\ -(c_{13} + c_{44}) & -c_{33} & e_{15} & q_{33} \\ (e_{15} + e_{31}) & e_{33} & \varepsilon_{11} & d_{33} \\ (q_{15} + q_{31}) & q_{33} & d_{11} & \mu_{33} \end{pmatrix} - c_{44}\det\begin{pmatrix} -c_{44} & e_{15} & q_{33} \\ e_{15} & \varepsilon_{11} & d_{33} \\ q_{15} & d_{11} & \mu_{33} \end{pmatrix} \\ & + \det\begin{pmatrix} -c_{11} & -(c_{13} + c_{44}) & (e_{15} + e_{31}) & 0 \\ -(c_{13} + c_{44}) & -c_{33} & e_{33} & q_{15} \\ (e_{15} + e_{31}) & e_{33} & \varepsilon_{33} & d_{11} \\ (q_{15} + q_{31}) & q_{33} & d_{33} & \mu_{11} \end{pmatrix} \\ & - c_{44}\det\begin{pmatrix} -c_{33} & e_{15} & q_{15} \\ e_{33} & \varepsilon_{11} & d_{11} \\ q_{33} & d_{11} & \mu_{11} \end{pmatrix}. \end{aligned} \tag{A10c}$$

Other coefficients in (A4a) and (A4b) are defined as

$$\begin{cases} m_{nj} = -\Lambda_{n;1(j+1)}/\Lambda_{n;11}, \quad \alpha_{nj} = m_{nj}s_n, \\ \theta_{nj} = C_{j+2} + \sum_{k=1}^{3} C_{jk}m_{nk}, \quad \omega_{nj} = \theta_{nj}s_n \quad (n = 1, 2, 3, 4), \end{cases} \tag{A11}$$

where $\Lambda_{n;pq}$ (n, p, $q = 1, 2, 3, 4$) are the cofactors of the pq element of the matrix $\mathbf{\Pi}_n$ defined by (A8); C_{ij} is the element of a symmetric matrix defined by

$$(C_{ij})_{3\times3} = \begin{pmatrix} c_{44} & e_{15} & q_{15} \\ e_{15} & -\varepsilon_{11} & -d_{11} \\ q_{15} & -d_{11} & -\mu_{11} \end{pmatrix}, \tag{A12a}$$

and C_J is defined by

$$C_J = \begin{cases} c_{44}, & J = 1, 2, 3, \\ e_{15}, & J = 4, \\ q_{15}, & J = 5. \end{cases} \tag{A12b}$$

Obviously, we have $C_{1j} = C_{j1} = C_{j+2}$.

Notice that m_{nj} (n=1, 2, 3, 4) satisfy the following relation:

$$\mathbf{\Pi}_n \begin{pmatrix} -1 & m_{n1} & m_{n2} & m_{n3} \end{pmatrix}^{\mathrm{T}} = \mathbf{0}_{4\times1} \quad (n = 1, 2, 3, 4), \tag{A13}$$

in which "T" denotes the transpose of a matrix or a vector.

Moreover, we have the following relations:

$$\begin{cases} \sum_{n=1}^{4} s_n H_n = 1, \quad \sum_{n=1}^{4} s_n H_n m_{ni} = 0, \quad \sum_{n=1}^{4} s_n H_n \theta_{nj} = C_{j+2}, \\ \sum_{n=1}^{4} s_n H_n m_{ni}\theta_{nj} = \begin{cases} 0, & i \neq j, \\ -c_{44}, & i = j, \end{cases} \quad \sum_{n=1}^{4} s_n H_n \theta_{nj}\theta_{n1} = 0, \end{cases} \tag{A14}$$

which can be verified by direct substitutions. In (A14), H_n ($n = 1, 2, 3, 4$) are given by (10).

Appendix B Dislocation loops in transversely isotropic MEE half space with free surface

For arbitrarily shaped 3D dislocation loops in a transversely isotropic MEE half space with a free surface, the line-integral expressions given in (22), (27), (36), (44a), and (44b) are still applicable, provided that we make modifications to (11a) and (11b) according to the free-surface boundary condition, and then set $\lambda = \mu$=1 for the half space $x_3 \geqslant 0$ while $\lambda = \mu = 2$ for the half space $x_3 \leqslant 0$. Here, we also assume that the isotropic plane of the transversely isotropic material is parallel to the free surface of the half space (i.e., the x_1x_2-plane).

The free-surface boundary condition means the vanishing of the extended stresses σ_{3J} at $x_3 = 0$, which gives, corresponding to (11a) and (11b), that

$$p_{55}^{[\mu][\mu]} = 1, \tag{B1a}$$

and

$$\begin{pmatrix} p_{1n}^{[\mu][\mu]} \\ p_{2n}^{[\mu][\mu]} \\ p_{3n}^{[\mu][\mu]} \\ p_{4n}^{[\mu][\mu]} \end{pmatrix} = \begin{pmatrix} \omega_{11}^{[\mu]} & \omega_{21}^{[\mu]} & \omega_{31}^{[\mu]} & \omega_{41}^{[\mu]} \\ \theta_{11}^{[\mu]} & \theta_{21}^{[\mu]} & \theta_{31}^{[\mu]} & \theta_{41}^{[\mu]} \\ \theta_{12}^{[\mu]} & \theta_{22}^{[\mu]} & \theta_{32}^{[\mu]} & \theta_{42}^{[\mu]} \\ \theta_{13}^{[\mu]} & \theta_{23}^{[\mu]} & \theta_{33}^{[\mu]} & \theta_{43}^{[\mu]} \end{pmatrix}^{-1} \begin{pmatrix} \omega_{n1}^{[\mu]} \\ -\theta_{n1}^{[\mu]} \\ -\theta_{n2}^{[\mu]} \\ -\theta_{n3}^{[\mu]} \end{pmatrix} \quad (n = 1, 2, 3, 4). \tag{B1b}$$